STATISTICS, OPTIMIZATION AND INFORMATION COMPUTING
Stat., Optim. Inf. Comput., Vol. **x**, Month 202x, pp 0–44.
Published online in International Academic Press (www.IAPress.org)

Modeling Coupled Wasting-Stunting Dynamics and Chronic Undernutrition Persistence in Indonesia

Nur Rahmi [1,*], Wahyuni Ekasasmita [1], Ahmad Fajri S. [1], Muhammad Rifki Nisardi [2], Kusnaeni [1], Muhammad Fadhil Nurahmad [1]

[1] *Department of Science, Institut Teknologi Bacharuddin Jusuf Habibie, Indonesia*
[2] *Department of Production and Industrial Technology, Institut Teknologi Bacharuddin Jusuf Habibie, Indonesia*

Abstract Child undernutrition remains a major global public health challenge, with wasting and stunting representing acute and chronic manifestations of nutritional failure, respectively. Although strong epidemiological associations between wasting and stunting have been widely reported, the long-term dynamical mechanisms governing their interaction at the population level remain insufficiently understood. This study develops a coupled wasting–stunting dynamical model to investigate the interaction between acute and chronic undernutrition among children under five years of age in Indonesia. The proposed framework integrates wasting progression, severe wasting dynamics, chronic stunting accumulation, and nonlinear interaction mechanisms linking acute nutritional deterioration and chronic growth failure. The model additionally incorporates low birth weight recruitment as an early-life nutritional vulnerability mechanism. Model parameters were obtained through demographic assignment, literature-informed specification, empirical approximation, and semi-mechanistic calibration using Indonesian national nutritional surveillance data covering the period 2013–2024. The analytical results revealed a hierarchical dynamical structure governed by the wasting progression threshold $\mathcal{R}_W$. The analysis demonstrated that persistent wasting exposure may amplify long-term chronic undernutrition through nonlinear interaction pathways, while chronic growth failure simultaneously increases susceptibility to recurrent wasting progression. Local stability analysis showed that the wasting subsystem remains asymptotically stable under the calibrated parameter configuration satisfying $\mathcal{R}_W < 1$. Model robustness and parameter influence were further evaluated using profile likelihood analysis, bootstrap-based uncertainty assessment, local sensitivity analysis, and variance-based global sensitivity analysis using Sobol indices. The sensitivity analyses demonstrated that wasting dynamics are governed primarily by deterioration and recovery processes, whereas long-term stunting persistence is dominated mainly by baseline chronic progression mechanisms. Long-term projections under multiple intervention scenarios showed that recovery-oriented interventions substantially reduce wasting and severe wasting prevalence, but produce only relatively modest reductions in stunting prevalence over the period 2024–2045. Even under intensive intervention scenarios, the projected stunting prevalence remained above the national target threshold of 14%, indicating the presence of strong structural persistence within the chronic undernutrition subsystem. Overall, the study suggests that chronic undernutrition should not be interpreted merely as an isolated nutritional condition, but rather as an emergent population-level consequence of sustained nutritional exposure, nonlinear interaction dynamics, and long-term feedback accumulation. The proposed framework provides a quantitative basis for evaluating long-term nutritional intervention strategies in settings with limited longitudinal nutritional transition data.

Keywords Child malnutrition dynamics, Wasting, Stunting, Dynamical systems, Threshold analysis, Sobol sensitivity analysis, Profile likelihood, Semi-mechanistic calibration, Long-term projection

AMS 2010 subject classifications 92D30, 34A34, 37N25, 65C20, 62P10

DOI: 10.19139/soic-2310-5070-3543

1. Introduction

1.1. Problem background

Child undernutrition remains a major global public health concern despite extensive international efforts and large-scale intervention programs [1, 2, 3]. Nearly half of deaths among children under five years of age are associated

ISSN 2310-5070 (online) ISSN 2311-004X (print)

with undernutrition, reflecting the profound physiological vulnerability of affected children. Undernourished children face substantially elevated risks of severe infections and other medical complications due to impaired immune and developmental function, a pattern also observed across multiple patient populations [4, 5, 6, 7, 8]. As such, undernutrition represents not only a clinical issue but also a long-term constraint on socioeconomic development

Two major anthropometric indicators used to describe childhood undernutrition are wasting and stunting. Wasting (low weight-for-height) reflects acute nutritional stress, whereas stunting (low height-for-age) represents cumulative growth failure arising from prolonged nutritional deprivation [9]. Although operationally treated as distinct indicators, empirical evidence increasingly suggests that these conditions are dynamically linked [10, 11, 12, 13, 14]. Longitudinal studies show that early-life wasting episodes significantly increase the risk of subsequent stunting, while repeated exposure amplifies this effect [15, 16]. Conversely, stunted children may exhibit increased susceptibility to infection and environmental stress, raising the risk of future wasting. These findings indicate that stunting should not be interpreted solely as a static chronic condition, but rather as the cumulative outcome of prior acute malnutrition processes

Despite growing evidence supporting the biological linkage between wasting and stunting at the individual level, the extent to which wasting dynamics influence stunting prevalence at the population level remains unclear.In particular, it is not well understood whether wasting–stunting interactions play a dominant role in shaping long-term dynamics, or whether stunting is primarily driven by baseline structural factors such as persistent nutritional conditions and demographic processes. In many settings, wasting prevalence decreases rapidly following therapeutic interventions while stunting prevalence declines slowly or stabilizes [3]. Longitudinal studies have shown that early-life wasting increases the risk of subsequent stunting, while repeated episodes may amplify long-term growth deficits [16]. Conversely, stunting has been associated with increased vulnerability to infections, potentially elevating the risk of future wasting [17]. However, despite these individual-level findings, the extent to which wasting dynamics contribute to stunting prevalence at the population level remains unclear. This uncertainty is further complicated by differences in temporal dynamics: wasting responds rapidly to short-term interventions, whereas stunting evolves more slowly due to its cumulative nature. As a result, improvements in acute malnutrition do not necessarily translate into proportional reductions in chronic growth failure.

This ambiguity has direct implications for public health policy. Many nutrition programs prioritize the reduction of wasting through targeted interventions, such as supplementary feeding and therapeutic treatment. While these approaches can produce rapid improvements in acute malnutrition, their long-term impact on stunting reduction remains uncertain [18]. In Indonesia, recent efforts have led to gradual reductions in stunting prevalence, yet the rate of decline remains relatively slow compared to fluctuations observed in wasting [19, 20, 21, 22]. This raises a fundamental policy question: whether interventions targeting wasting are sufficient to achieve long-term stunting reduction targets, or whether deeper structural changes are required.

Mathematical modeling provides a systematic framework to address complex problems by formalizing relevant processes and interactions into quantitative systems that can be analyzed, interpreted, and optimized. Such approaches have been widely applied across various fields, including biological and epidemiological studies as well as financial optimization and decision-making systems [23, 24]. Within this framework, observed prevalence—defined through WHZ- and HAZ-based classifications—is interpreted not as a collection of independent measurements, but as the aggregate outcome of continuous transitions between nutritional states over time. Such an approach enables the identification of latent mechanisms governing population dynamics, the estimation of transition processes from available data, and the evaluation of intervention scenarios beyond those directly observed. Consequently, mathematical models serve as a bridge between empirical trends and underlying system behavior, offering insights that extend beyond descriptive statistical analysis.

Against this backdrop, the persistent disparity between rapid improvements in wasting and slower declines in stunting raises an important policy-relevant question: to what extent do reductions in wasting translate into sustained reductions in stunting at the population level? This suggests that the interaction between wasting and stunting may involve intrinsic dynamical mechanisms that cannot be fully captured through descriptive statistical analysis alone. Consequently, a mathematical modeling approach is needed to investigate how transitions between nutritional states shape long-term population outcomes and intervention effectiveness. Taken together, these issues

highlight the need for a deeper investigation into the dynamical relationship between wasting and stunting and the extent to which current modeling approaches capture their long-term population behavior.

1.2. Related work and positioning of the present study

Quantitative studies on child undernutrition have been developed using statistical, epidemiological, and mechanistic dynamical approaches. While these approaches provide complementary insights, their ability to capture the structural drivers of long-term stunting dynamics remains limited. Statistical and machine learning models are primarily designed for prediction and risk classification. For instance, nonparametric regression approaches using spline and Fourier estimators have demonstrated strong predictive performance in modeling stunting prevalence [25]. The study demonstrates strong predictive performance, as indicated by low Generalized Cross Validation (GCV) values and a high coefficient of determination. However, the model is formulated as a direct mapping from covariates to observed prevalence, which prevents the disentanglement of underlying population processes. In particular, it cannot distinguish whether observed changes in stunting arise from variations in incidence, recovery, or delayed effects of prior nutritional conditions. As a result, the approach is not suitable for analyzing transition dynamics or evaluating the long-term impact of interventions beyond observed data patterns.

A machine learning-based approach using the k-nearest neighbor (k-NN) algorithm has been developed in [26] to predict the risk of stunting in newborns. This model improves classification accuracy and supports early detection of at-risk individuals. Nevertheless, its predictive nature remains purely data-driven, without embedding biological or epidemiological structure. Consequently, it does not provide insight into how nutritional states evolve over time, nor does it allow simulation of counterfactual intervention scenarios, limiting its relevance for long-term policy analysis.

From an epidemiological perspective, observational and cohort-based analyses in [10] provide robust empirical evidence on the relationship between wasting and stunting. These studies consistently show that the two conditions frequently coexist and that wasting significantly increases the risk of subsequent stunting. While such findings establish a clear temporal and causal linkage at the individual level, they do not translate into a predictive population-level framework. In particular, epidemiological models do not formalize how these risk relationships aggregate into dynamic transitions across nutritional states, leaving the mechanisms driving long-term prevalence patterns unresolved.

Motivated by this limitation, mechanistic modeling approaches have been developed to explicitly represent transitions between nutritional states. A modified SEIR-type compartmental model has been introduced in [27], incorporating both child and maternal compartments to account for socio-demographic influences such as maternal education. Although this framework enhances structural interpretability, it does not explicitly model the interaction between wasting and stunting as a coupled dynamical process, thereby limiting its ability to capture the pathway linking acute and chronic malnutrition. A related compartmental framework has been proposed in [28], categorizing the population into at-risk, stunted, and intervention states to evaluate program effectiveness using regional data. While suitable for assessing intervention outcomes, the model adopts a simplified state structure that does not represent the multi-stage progression from wasting to stunting. As a consequence, it cannot distinguish whether persistent stunting is driven by ongoing incidence, incomplete recovery, or delayed effects of prior wasting episodes, which are central to understanding long-term system behavior. Extending beyond compartmental formulations, a System Dynamics (SD) model has been developed in [29] to describe transitions across body mass index (BMI) categories within different socioeconomic strata. This approach captures feedback mechanisms and broader structural determinants of nutritional status. However, the reliance on BMI-based classification introduces a fundamental limitation, as it does not align with standard anthropometric indicators used to define wasting (WHZ) and stunting (HAZ). Consequently, the model operates on an aggregated proxy that cannot distinguish acute and chronic malnutrition or represent biologically meaningful transition pathways. In addition, its reliance on heuristic parameterization and limited calibration against prevalence data, combined with the absence of identifiability analysis, constrains its ability to generate reliable quantitative projections for policy evaluation.

Taken together, these studies reveal a consistent and multi-layered methodological gap. Statistical and machine learning models provide high predictive accuracy but lack mechanistic interpretability and temporal structure. Epidemiological studies establish causal relationships but do not provide a predictive dynamical framework.

Existing mechanistic models capture system dynamics but rely on simplified state representations, omit explicit wasting–stunting coupling, and often employ calibration strategies that are not fully consistent with available data structures. More fundamentally, issues of data consistency and parameter identifiability remain largely unaddressed. Most available nutrition datasets consist of repeated cross-sectional prevalence estimates rather than longitudinal trajectories, yet many models are formulated in absolute population terms without accounting for this limitation. This mismatch introduces scaling inconsistencies during calibration and allows multiple parameter combinations to produce indistinguishable outputs, thereby reducing interpretability and weakening policy relevance. These limitations indicate the absence of an integrated modeling framework that simultaneously: (i) represents multi-stage nutritional dynamics, (ii) explicitly captures the coupling between wasting and stunting, (iii) remains consistent with the structure of available population-level data, and (iv) ensures identifiable parameter inference. Addressing this gap motivates the development of a data-consistent and mechanistically interpretable modeling framework.

Building upon the limitations identified in previous studies, the present work is positioned as a data-driven and mechanism-oriented extension of existing dynamical modeling approaches for child undernutrition. While prior models have primarily focused on structural representation or intervention evaluation, they have not systematically assessed the relative importance of competing mechanisms within the system. In contrast, this study is designed not only to represent the dynamics of undernutrition, but also to quantitatively evaluate which mechanisms truly govern long-term stunting prevalence at the population level. This shift from structural modeling to mechanism identification constitutes the central motivation of the study.

From a structural perspective, the proposed model integrates wasting and stunting within a unified dynamical framework, allowing simultaneous representation of acute and chronic undernutrition processes. The model captures the multi-stage progression of wasting through transitions between normal, wasting, and severe wasting states, while chronic growth failure is represented through a coupled stunting subsystem. In addition, the framework incorporates biologically important early-life vulnerability factors, particularly low birth weight (LBW), which has been consistently associated with elevated risks of wasting, impaired catch-up growth, and persistent stunting during early childhood [30, 31]. Rather than introducing explicit birth compartments, these early-life structural vulnerabilities are incorporated implicitly through the chronic progression dynamics of the model.

The interaction between wasting and stunting is represented through a nonlinear hazard-based mechanism that allows persistent wasting exposure to amplify the effective progression toward chronic growth failure, while chronic undernutrition simultaneously increases susceptibility to recurrent wasting progression. This coupled structure enables the model to capture reinforcing feedback mechanisms between acute and chronic malnutrition without imposing deterministic transitions between nutritional states.

From a methodological standpoint, the study adopts a fully data-consistent approach based on aggregate national prevalence observations. Time-varying inputs are constructed through interpolation of empirical nutritional data, while model parameters are identified using calibration procedures aligning simulated trajectories with observed prevalence patterns. To ensure robustness, interpretability, and practical identifiability, the model is evaluated using a comprehensive analytical framework consisting of threshold analysis, profile likelihood analysis, local sensitivity analysis (LSA), and global sensitivity analysis based on Sobol indices.

A key novelty of this study lies not only in the construction of a coupled wasting–stunting dynamical system, but also in the identification of the dominant mechanisms governing long-term chronic undernutrition persistence. By integrating calibration, threshold analysis, and sensitivity analysis within a unified framework, the study demonstrates that long-term stunting dynamics are governed predominantly by baseline chronic progression mechanisms, whereas wasting-related interaction effects contribute primarily as secondary amplification pathways at the population level. This finding provides a rigorous basis for understanding the hierarchical structure of undernutrition persistence and explains why reductions in acute malnutrition burden do not necessarily translate immediately into rapid declines in chronic stunting prevalence.

Finally, the model is used to perform long-term numerical projections under multiple intervention scenarios, allowing evaluation of realistic policy trajectories for nutritional improvement. The projection results reveal an important structural insight: although intervention intensification substantially reduces wasting and severe wasting prevalence, long-term stunting reduction remains comparatively slow because the chronic undernutrition subsystem

exhibits strong structural persistence and long temporal memory. Consequently, even when theoretical equilibrium reductions are achievable, the convergence dynamics of the system may prevent policy targets from being reached within realistic intervention time horizons.

Through this integrated analytical framework, the present study contributes not only a more comprehensive mathematical representation of wasting–stunting interaction dynamics, but also a deeper mechanistic understanding of the dominant drivers governing long-term undernutrition persistence. By combining structural epidemiological realism with mechanism identification and long-term policy projection, the study addresses an important gap in the existing literature and provides a stronger quantitative foundation for evidence-based nutritional intervention planning.

1.3. Research Question, Key Findings, and Implications

Based on the proposed modeling framework, this study is guided by the following central research question:

"To what extent do wasting dynamics contribute to long-term stunting prevalence, and can reductions in wasting alone achieve stunting reduction targets?"

This question arises from the gap between empirical evidence at the individual level and the unclear role of wasting–stunting interactions at the population level. While previous studies suggest a potential linkage between the two conditions, their relative contribution within a dynamical system has not been rigorously quantified.

By addressing this question through a data-driven dynamical model combined with calibration, identifiability analysis, and both local and global sensitivity analysis, this study provides a key insight: the contribution of wasting-related mechanisms to stunting dynamics is comparatively limited at the population level, whereas baseline structural factors play a more dominant role. This finding challenges the common assumption that reducing acute malnutrition alone is sufficient to drive long-term improvements in stunting prevalence.

From a modeling perspective, the results demonstrate that complex multi-compartment systems can be systematically simplified when supported by sensitivity and identifiability analysis. In particular, the identification of dominant parameters enables a principled reduction of the model without loss of essential dynamical behavior. This highlights the importance of integrating model calibration with sensitivity analysis to avoid unnecessary structural complexity.

From a policy perspective, the findings suggest that interventions focusing solely on wasting reduction may not be sufficient to achieve long-term stunting targets. Instead, effective strategies should address underlying structural determinants, such as persistent nutritional conditions and early-life risk factors. Moreover, the projection results indicate that even when equilibrium targets are theoretically attainable, the convergence dynamics of the system may delay their realization within practical policy time horizons.

2. Mathematical model

2.1. Overall modeling framework and subsystem structure

This study employs a population-based mathematical modeling framework to investigate the long-term dynamics of child nutritional status among children under five years of age. The model is designed to capture the interaction between acute malnutrition (wasting) and chronic growth impairment (stunting), and to evaluate the long-term population-level impact of community-based nutrition interventions.

Because the available data consist primarily of repeated cross-sectional prevalence estimates rather than individual longitudinal trajectories, the model is formulated at the population level. All state variables represent population counts, and model parameters are interpreted as effective transition rates summarizing average population dynamics. Time is measured in yearly units, consistent with the temporal resolution of national nutrition surveillance data and administrative program records.

To ensure consistency with national anthropometric indicators and to avoid double counting arising from overlapping nutritional classifications, the model is decomposed into two causally linked but structurally distinct subsystems. The first subsystem represents acute nutritional status based on the weight-for-height (WHZ) indicator and captures short-term changes in body weight, including growth faltering and wasting. The second subsystem

represents chronic nutritional status based on the height-for-age (HAZ) indicator and captures long-term linear growth impairment. The interaction between the two subsystems is modeled through population-level risk modulation rather than explicit individual flows, allowing wasting prevalence to influence stunting incidence and progression while preserving consistency with cross-sectional surveillance data.

2.2. Model assumptions

The model is developed under the following assumptions:

(i) **Population-based representation.** The model describes nutritional dynamics at the population level. All state variables represent aggregated population counts, and transition rates reflect average population processes rather than individual nutritional trajectories. Individual heterogeneity, repeated wasting episodes, and within-child histories are not explicitly modeled.

(ii) **Open population system.** The under-five population is modeled as an open system with continuous inflow through live births and outflow through natural mortality and aging beyond five years. The aging-out process is assumed to occur at a constant rate across all nutritional states.

(iii) **Low birth weight as an initiating growth deficit.** Although weight-for-height indicators are not defined at birth, newborns with low birth weight (LBW) are represented as entering the growth faltering pathway as a population-level abstraction of early deviation from optimal growth trajectories. LBW is therefore not interpreted as wasting at birth nor modeled as a separate compartment, but as an initial condition that elevates the subsequent risk of wasting and stunting in early childhood [30]. This formulation allows the model to incorporate empirically observed early-life vulnerability while maintaining consistency with anthropometric definitions.

(iv) **Recovery dynamics.** Recovery and transition processes are modeled using a continuous-time stochastic (Poisson-type) framework, where transitions are interpreted as event intensities. Recovery rates depend on disease severity, with substantially lower recovery intensity observed in severely wasted children [16, 32].

(v) **Reversible stunting with early-life constraint.** Stunting is modeled as a partially reversible condition within the time horizon considered, allowing transition from stunted to non-stunted states through catch-up linear growth, but primarily restricted to early childhood. Evidence indicates that linear growth faltering occurs early in life and that height-for-age deficits established during this period tend to persist, with only limited catch-up growth observed after infancy. Although nutritional interventions can improve growth outcomes, improvements in height-for-age are typically modest compared to weight-based recovery indicators [18]. Longitudinal cohort evidence further confirms that recovery in linear growth is incomplete for a large proportion of children even after nutritional improvements [33]. Accordingly, stunting recovery is modeled as a low-intensity transition process constrained to early developmental windows.

(vi) **Interaction between wasting and stunting.** The interaction between wasting and stunting is modeled using a relative risk framework, where each condition increases the risk of the other through modulation of transition intensities. This bidirectional relationship reflects the synergistic effects of acute and chronic undernutrition mediated by infection, inflammation, and metabolic stress. Large-scale epidemiological evidence shows a substantial overlap between wasting and stunting, with strong age dependence and significant associations with infectious morbidity [34]. This supports modeling WaSt as a dynamic interaction rather than independent static conditions, preserving the probabilistic nature of co-occurrence in under-five populations.

(vii) **Mortality Representation.** Mortality in the model is represented by a single all-cause natural death rate that captures overall mortality in the under-five population. The model does not explicitly distinguish cause-specific mortality attributable to different nutritional compartments. This assumption is supported by evidence indicating that malnutrition contributes to mortality primarily in an indirect manner by increasing susceptibility to and severity of infectious diseases rather than acting as a direct cause of death, with consistent findings showing elevated mortality risk among malnourished children across infectious conditions and settings [35, 36]. From a modeling perspective, separating malnutrition-specific mortality from other causes is challenging in aggregated surveillance data, and introducing multiple cause-specific mortality parameters may lead to identifiability issues and overparameterization when only prevalence-level data are

available. Therefore, a single effective mortality parameter is used to ensure parsimony and consistency with data availability, while the increased mortality risk associated with malnutrition is implicitly captured at the population level.

(viii) **Near-Stationary Population Assumption.** For model normalization, the population is assumed to be in a near-stationary state, where the recruitment rate is approximately balanced by the total population outflow (including death and aging). This assumption is consistent with modern demographic theory based on the Stationary Population Identity (SPI), which relates observed populations to their stationary counterparts and characterizes deviations from structural equilibrium using age-structure and longevity dynamics [37, 38]. Recent developments in population dynamics further show that many populations exhibit convergence toward structural stationarity when analyzed through SPI-based frameworks, where deviations from stationarity can be quantified across age distribution, population momentum, and survival structure [38]. In epidemic modeling, analogous equilibrium assumptions are widely used, where long-term dynamics are studied in terms of stationary distributions or invariant measures under stochastic or deterministic frameworks [39, 40]. This normalization approach is commonly adopted in prevalence-based compartmental models to remove dependence on absolute population size and to focus on proportional dynamics. Additionally, it improves numerical stability in long-term simulations by preventing unbounded growth or decay of total population variables.

2.3. Model Formulation

Let $P(t)$ denote the total under-five population at time t, defined as

$$P(t) = O(t) + N(t) + W(t) + SW(t). \tag{1}$$

Wasting Subsystem. The dynamics of acute nutritional status are governed by the following system of ordinary differential equations:

$$\frac{dO}{dt} = \gamma_{NO}N - \gamma_{ON}O - (\mu+\delta)O, \tag{2}$$

$$\frac{dN}{dt} = \Lambda_N + \gamma_{ON}O - \gamma_{NO}N - \gamma_{NW}N + \phi_W W - (\mu+\delta)N, \tag{3}$$

$$\frac{dW}{dt} = \Lambda_W + \gamma_{NW}(1+\eta S)N - \gamma_{WS}W - \phi_W W - (\mu+\delta)W, \tag{4}$$

$$\frac{dSW}{dt} = \gamma_{WS}W - \phi_{SW}SW - (\mu+\delta)SW. \tag{5}$$

The recruitment terms satisfy

$$\Lambda_N = q_N\Lambda, \quad \Lambda_W = q_W\Lambda, \quad q_N + q_W = 1, \tag{6}$$

where Λ denotes the total birth rate. Since weight-for-height is not defined at birth, newborns are not classified anthropometrically. Instead, low birth weight is represented as an elevated initial risk of entering the wasting compartment. The term $\gamma_{NW}(1+\eta S)$ represents the increased risk of transition from normal to wasting in the presence of stunting. This formulation corresponds to a multiplicative relative risk effect, where $\eta = RR_{S\to W} - 1$, such that stunting proportionally amplifies the baseline transition rate γ_{NW}.

Stunting Subsystem. The dynamics of stunting are modeled as

$$\frac{dS}{dt} = \lambda_0\left(1 + \alpha\frac{W+SW}{P}\right)(1-S) - (\phi_S + \mu + \delta)S. \tag{7}$$

Here, $(W+SW)/P$ represents the prevalence of acute malnutrition in the population. The parameter

$$\alpha = RR_{W\to S} - 1$$

quantifies the increased risk of stunting associated with wasting conditions, implying a multiplicative relative risk effect on the baseline incidence rate λ_0.

The model assumes that stunting is partially reversible. The parameter ϕ_S denotes the recovery rate from stunting through catch-up linear growth, which reduces the proportion of stunted children and implicitly returns recovered individuals to the non-stunted population class at the aggregate level. Since the model is formulated in terms of population prevalence rather than explicit stunting-state compartments, recovery is represented as a reduction in the stunted proportion. This recovery process is assumed to occur primarily during early childhood, particularly within the first years of life, and becomes substantially less likely at older ages. Consequently, the combined term $(\phi_S + \mu + \delta)S$ represents the total rate of exit from the stunted state due to recovery, natural mortality, and demographic removal.

Dimensional consistency. All model equations are dimensionally consistent. State variables represent population counts (number of children), while time is measured in years. Accordingly, all transition, incidence, and recovery parameters are expressed in units of year^{-1}, ensuring that each term in the differential equations has units of children per year. Dimensionless quantities include population proportions and relative risk parameters. This consistency guarantees mathematical validity and facilitates interpretation of parameter magnitudes within an epidemiological framework.

2.3.1. Recovery Transition Intensities Recovery from wasting, severe wasting, and stunting is modeled as a stochastic transition process consistent with a Poisson framework, where nutritional recovery occurs continuously over time with constant effective transition intensities. Under this formulation, recovery parameters are interpreted as effective population-level recovery intensities.

Let r_X denote the observed recovery proportion associated with nutritional condition $X \in \{W, SW, S\}$. Assuming a Poisson transition mechanism, the effective recovery intensity is defined by

$$\phi_X = -\ln(1 - r_X). \tag{8}$$

where

- ϕ_W denotes the effective wasting recovery intensity,
- ϕ_{SW} denotes the effective severe wasting recovery intensity,
- ϕ_S denotes the effective stunting recovery intensity.

The resulting parameters represent effective population-level recovery processes incorporating not only therapeutic nutritional improvement itself, but also broader mechanisms such as intervention coverage, treatment accessibility, delayed diagnosis, household compliance, environmental conditions, and persistence of chronic developmental impairment. Distinct recovery intensities are specified for different nutritional conditions in order to reflect heterogeneity in biological severity and recovery mechanisms. In general, recovery from wasting is expected to occur more rapidly than recovery from severe wasting and chronic stunting, whereas recovery from stunting remains comparatively limited because of its cumulative developmental nature and restricted catch-up growth potential at the population level.

2.3.2. Model parameters The model consists of demographic, biological progression, intervention, and coupling parameters describing transitions between nutritional states. Table 1 lists all symbols together with their biological interpretation and units. This section introduces the mathematical structure of the model only, while the numerical values and identification procedures are presented later in Section 4 after parameter estimation and calibration.

Table 1 summarizes the parameters of the wasting–stunting model.

Table 1. Model parameters and definitions.

Symbol	Description	Unit
Demographic parameters		
Λ	Total recruitment rate (live births) into the under-five population	children·year^{-1}
μ	Natural mortality rate	year^{-1}
δ	Aging-out rate (exit at age five)	year^{-1}
Birth distribution		
q_N	Proportion of newborns entering the normal compartment	–
q_W	Proportion of newborns entering the wasting compartment (LBW proxy)	–
$\Lambda_N = q_N\Lambda$	Recruitment flow into normal state	children·year^{-1}
$\Lambda_W = q_W\Lambda$	Recruitment flow into wasting state	children·year^{-1}
Wasting transitions		
γ_{NO}	Transition rate from normal to overweight	year^{-1}
γ_{ON}	Transition rate from overweight to normal	year^{-1}
γ_{NW}	Transition rate from normal to wasting	year^{-1}
γ_{WS}	Transition rate from wasting to severe wasting	year^{-1}
Recovery dynamics		
r_W	Observed recovery proportion for wasting	–
r_{SW}	Observed recovery proportion for severe wasting	–
r_S	Observed recovery proportion for stunting	–
ϕ_W	Effective recovery intensity from wasting to normal	year^{-1}
ϕ_{SW}	Effective recovery intensity from severe wasting to wasting	year^{-1}
ϕ_S	Effective recovery intensity from stunting to non-stunted state	year^{-1}
Stunting dynamics		
λ_0	Baseline incidence rate of stunting	year^{-1}
$S(t)$	Proportion of stunted children	–
Interaction parameters		
α	Effect of wasting on stunting risk ($\alpha = RR_{W\to S} - 1$)	–
η	Effect of stunting on wasting risk ($\eta = RR_{S\to W} - 1$)	–

2.3.3. Model Standardization To align the model with prevalence-based data, all state variables are normalized by the total under-five population $P(t)$. Specifically, we define

$$o(t) = \frac{O(t)}{P(t)}, \quad n(t) = \frac{N(t)}{P(t)}, \quad w(t) = \frac{W(t)}{P(t)}, \quad sw(t) = \frac{SW(t)}{P(t)}, \quad s(t) = \frac{S(t)}{P(t)}. \tag{9}$$

The wasting-related compartments satisfy the conservation constraint

$$o(t) + n(t) + w(t) + sw(t) = 1, \tag{10}$$

while the stunting proportion satisfies

$$0 \le s(t) \le 1. \tag{11}$$

Under this normalization, the proportion of children experiencing acute malnutrition is given by

$$\frac{W(t) + SW(t)}{P(t)} = w(t) + sw(t). \tag{12}$$

Assuming a near-stationary population, the recruitment rate balances total outflow:

$$\lambda = \mu + \delta, \tag{13}$$

where λ denotes the effective per-capita recruitment rate.

This transformation yields a closed dynamical system in terms of proportions, eliminating dependence on absolute population size.

2.3.4. Final Standardized Model

Wasting Subsystem. The dynamics of acute nutritional status in normalized form are given by

$$\frac{do}{dt} = \gamma_{NO} n - \gamma_{ON} o - (\mu + \delta) o, \tag{14}$$

$$\frac{dn}{dt} = (1 - q_W)(\mu + \delta) + \gamma_{ON} o - \gamma_{NO} n - \gamma_{NW} n + \phi_W w - (\mu + \delta) n, \tag{15}$$

$$\frac{dw}{dt} = q_W (\mu + \delta) + \gamma_{NW}(1 + \eta s) n - \gamma_{WS} w - \phi_W w - (\mu + \delta) w, \tag{16}$$

$$\frac{dsw}{dt} = \gamma_{WS} w - \phi_{SW} sw - (\mu + \delta) sw. \tag{17}$$

Stunting Subsystem. The dynamics of chronic malnutrition are modeled as

$$\frac{ds}{dt} = \lambda_0 \left(1 + \alpha(w + sw)\right)(1 - s) - (\phi_S + \mu + \delta) s. \tag{18}$$

Model structure. The standardized system evolves on the feasible region

$$\Omega = \left\{ (o, n, w, sw, s) \in \mathbb{R}^5_+ : o + n + w + sw = 1,\ 0 \le s \le 1 \right\}. \tag{19}$$

This formulation ensures that all state variables represent proportions and remain bounded between 0 and 1. The interaction term $(w + sw)$ captures the prevalence of acute malnutrition, which modulates the incidence of stunting through a multiplicative effect governed by α.

The normalized system provides a mathematically consistent and epidemiologically interpretable framework for analyzing the coupled dynamics of wasting and stunting, and will be used in all subsequent analytical developments.

3. Mathematical Analysis of the Model

In this section, we analyze the mathematical properties of the standardized wasting–stunting model, including well-posedness, positivity, and boundedness. All parameters are assumed to be nonnegative.

3.1. Positivity and Well-Posedness

Lemma 3.1. *For any initial condition $(o(0), n(0), w(0), sw(0), s(0)) \in \Omega$, where*

$$\Omega = \left\{ (o, n, w, sw, s) \in \mathbb{R}^5_+ :\ o + n + w + sw = 1,\ 0 \le s \le 1 \right\},$$

the standardized wasting–stunting model admits a unique global solution for all $t \ge 0$.

Proof
Let $X(t) = (o, n, w, sw, s)^\top$. Then the system can be written compactly as

$$\frac{dX}{dt} = F(X),$$

with

$$\begin{aligned}
F_1 &= \gamma_{NO} n - \gamma_{ON} o - (\mu + \delta) o, \\
F_2 &= (1 - q_W)(\mu + \delta) + \gamma_{ON} o - \gamma_{NO} n - \gamma_{NW} n + \phi_W w - (\mu + \delta) n, \\
F_3 &= q_W(\mu + \delta) + \gamma_{NW}(1 + \eta s) n - \gamma_{WS} w - \phi_W w - (\mu + \delta) w, \\
F_4 &= \gamma_{WS} w - \phi_{SW} sw - (\mu + \delta) sw, \\
F_5 &= \lambda_0(1 + \alpha(w + sw))(1 - s) - (\phi_S + \mu + \delta) s.
\end{aligned}$$

Since each component $F_i(X)$ is continuously differentiable on Ω, the vector field F is locally Lipschitz continuous. Hence, by the Picard–Lindelöf theorem, the system admits a unique local solution for every initial condition in Ω. Furthermore, the solution remains bounded inside Ω by positive invariance established below, implying existence of a unique global solution for all $t \geq 0$. □

Lemma 3.2. *The region Ω is positively invariant.*

Proof
We verify that the vector field points inward on the boundary of Ω. If $o = 0$, then $\frac{do}{dt} = \gamma_{NO} n \geq 0$. If $n = 0$, then $\frac{dn}{dt} = (1 - q_W)(\mu + \delta) + \gamma_{ON} o + \phi_W w \geq 0$. If $w = 0$, then $\frac{dw}{dt} = q_W(\mu + \delta) + \gamma_{NW}(1 + \eta s) n \geq 0$. If $sw = 0$, then $\frac{dsw}{dt} = \gamma_{WS} w \geq 0$. If $s = 0$, then $\frac{ds}{dt} = \lambda_0(1 + \alpha(w + sw)) \geq 0$, while for $s = 1$, $\frac{ds}{dt} = -(\phi_S + \mu + \delta) \leq 0$.

Hence, the vector field points inward or tangentially on every boundary component of Ω. Therefore, Ω is positively invariant. □

Lemma 3.3. *All solutions remain bounded in the feasible region Ω for all $t \geq 0$.*

Proof
By construction, $o + n + w + sw = 1$, so the wasting subsystem evolves on the unit simplex. For the stunting variable,

$$\frac{ds}{dt} = \lambda_0(1 + \alpha(w + sw))(1 - s) - (\phi_S \mu + \delta) s.$$

Since $0 \leq w + sw \leq 1$, we have

$$\frac{ds}{dt} \leq \lambda_0(1 + \alpha)(1 - s).$$

Thus $s(t)$ remains bounded in $[0, 1]$. Therefore, all solutions remain in Ω. □

3.2. Equilibria of the Model

An equilibrium point of the system is obtained by setting all time derivatives equal to zero. Biologically, an equilibrium represents a long-term steady-state nutritional composition of the under-five population in terms of prevalence proportions.

3.3. Equilibrium Points

The model admits a biologically meaningful wasting-free equilibrium, while complete elimination of chronic undernutrition is generally not achievable because of persistent baseline progression toward stunting.

3.3.1. Wasting-Free Equilibrium The wasting-free equilibrium corresponds to the state in which wasting and severe wasting are absent:

$$w^* = sw^* = 0.$$

Substituting these conditions into (14) and (15) gives

$$0 = \gamma_{NO} n^* - \gamma_{ON} o^* - (\mu + \delta) o^*, \tag{20}$$
$$0 = (1 - q_W)(\mu + \delta) + \gamma_{ON} o^* - \gamma_{NO} n^* - (\mu + \delta) n^*. \tag{21}$$

Solving the system yields

$$n^* = 1 - q_W,$$

and

$$o^* = \frac{\gamma_{NO}}{\gamma_{ON} + \mu + \delta}(1 - q_W).$$

The equilibrium stunting level is obtained from (18):

$$0 = \lambda_0(1 - s^*) - (\phi_S + \mu + \delta)s^*,$$

which gives

$$s^* = \frac{\lambda_0}{\lambda_0 + \phi_S + \mu + \delta}.$$

Therefore, the wasting-free equilibrium is

$$E_W = (o^*, n^*, 0, 0, s^*), \tag{22}$$

where

$$n^* = 1 - q_W, \qquad o^* = \frac{\gamma_{NO}}{\gamma_{ON} + \mu + \delta}(1 - q_W),$$

and

$$s^* = \frac{\lambda_0}{\lambda_0 + \phi_S + \mu + \delta}.$$

Biological interpretation. The equilibrium E_W represents a population state in which acute malnutrition has been eliminated, while chronic undernutrition persists at a positive endemic level. The equilibrium stunting prevalence is determined by the balance between baseline chronic progression and effective recovery dynamics. Thus, even in the absence of wasting and severe wasting, the system may still converge to a nonzero chronic undernutrition equilibrium because of persistent structural inflow into the stunting compartment.

3.3.2. Stunting-Free Equilibrium A stunting-free equilibrium would require

$$s^* = 0.$$

Evaluating (18) at $s = 0$ gives

$$\left.\frac{ds}{dt}\right|_{s=0} = \lambda_0\big(1 + \alpha(w + sw)\big).$$

Since all parameters and state variables are nonnegative,

$$\left.\frac{ds}{dt}\right|_{s=0} > 0 \qquad \text{whenever } \lambda_0 > 0.$$

Therefore, the system does not admit a biologically meaningful stunting-free equilibrium under positive baseline chronic progression intensity. Persistent inflow into the stunting compartment continuously generates chronic undernutrition, preventing complete elimination of stunting at equilibrium.

Consequently, the model also does not admit a biologically meaningful undernutrition-free equilibrium whenever $\lambda_0 > 0$. Even if wasting and severe wasting are absent, the system still converges toward a positive endemic stunting level determined by the balance between chronic progression and recovery processes. Hence, the wasting-free equilibrium E_W represents the lowest biologically attainable equilibrium state of the system under persistent baseline chronic undernutrition pressure.

3.4. Threshold around the wasting-free equilibrium E_W

When $\lambda_0 > 0$, the system admits the wasting-free equilibrium E_W given in (22). Near E_W, the stunting prevalence remains close to s^*, so the wasting progression term becomes

$$\gamma_{NW}(1+\eta s) \approx \gamma_{NW}(1+\eta s^*).$$

The corresponding linearized subsystem is

$$\frac{d}{dt}\begin{pmatrix} w \\ sw \end{pmatrix} = (\mathbf{F}_W - \mathbf{V})\begin{pmatrix} w \\ sw \end{pmatrix},$$

where

$$\mathbf{F}_W = \begin{pmatrix} \gamma_{NW}(1+\eta s^*)n^* & 0 \\ 0 & 0 \end{pmatrix},$$

and

$$\mathbf{V} = \begin{pmatrix} \mu+\delta+\phi_W & 0 \\ -\gamma_{WS} & \mu+\delta+\phi_{SW} \end{pmatrix}.$$

The next-generation operator is

$$\mathbf{K}_W = \mathbf{F}_W\mathbf{V}^{-1},$$

which yields

$$\mathbf{K}_W = \begin{pmatrix} \dfrac{\gamma_{NW}(1+\eta s^*)n^*}{\mu+\delta+\phi_W} & 0 \\ 0 & 0 \end{pmatrix}.$$

Therefore, the wasting progression threshold around E_W is

$$\mathcal{R}_W = \frac{\gamma_{NW}(1+\eta s^*)n^*}{\mu+\delta+\phi_W} = \frac{\gamma_{NW}(1+\eta s^*)(1-q_W)}{\mu+\delta+\phi_W}. \tag{23}$$

The quantity $\mathcal{R}_W$ represents the effective amplification potential of wasting prevalence near the wasting-free equilibrium. The ratio $\frac{\gamma_{NW}}{\mu+\delta+\phi_W}$ describes the balance between wasting progression and removal through recovery or demographic turnover. The factor $(1-q_W)$ represents the proportion of children entering the population in the normal nutritional state and therefore remaining susceptible to wasting progression. Under persistent chronic undernutrition, the multiplicative term $(1+\eta s^*)$ captures the additional wasting susceptibility induced by background stunting prevalence. Consequently, chronic undernutrition amplifies the effective wasting progression threshold through increased nutritional vulnerability. Biologically, $\mathcal{R}_W < 1$ implies that wasting prevalence cannot sustain itself and gradually declines toward the wasting-free equilibrium, whereas $\mathcal{R}_W > 1$ implies persistence of acute undernutrition and emergence of endemic wasting dynamics.

Theorem 3.4. *Assume that $\lambda_0 > 0$. Then the wasting-free equilibrium E_W given in (22) is locally asymptotically stable if $\mathcal{R}_W < 1$, and unstable if $\mathcal{R}_W > 1$.*

Proof

Near E_W, the stunting prevalence remains close to s^*, so the wasting progression term (22) satisfies $\gamma_{NW}(1+$

$\eta s) \approx \gamma_{NW}(1+\eta s^*)$. The linearized wasting subsystem is

$$\frac{d\mathbf{x}}{dt} = (\mathbf{F}_W - \mathbf{V})\mathbf{x}, \qquad \mathbf{x} = (w, sw)^T,$$

where

$$\mathbf{F}_W = \begin{pmatrix} \gamma_{NW}(1+\eta s^*)n^* & 0 \\ 0 & 0 \end{pmatrix},$$

and

$$\mathbf{V} = \begin{pmatrix} \mu+\delta+\phi_W & 0 \\ -\gamma_{WS} & \mu+\delta+\phi_{SW} \end{pmatrix}.$$

The next-generation operator is

$$\mathbf{K}_W = \mathbf{F}_W \mathbf{V}^{-1}.$$

Since $\mathbf{K}_W$ is upper triangular, its eigenvalues are

$$\left\{ \frac{\gamma_{NW}(1+\eta s^*)n^*}{\mu+\delta+\phi_W}, 0 \right\}.$$

Using $n^* = 1 - q_W$, we obtain

$$\rho(\mathbf{K}_W) = \frac{\gamma_{NW}(1+\eta s^*)(1-q_W)}{\mu+\delta+\phi_W} = \mathcal{R}_W.$$

Therefore, by the standard next-generation stability criterion, the wasting-free equilibrium E_W is locally asymptotically stable whenever $\mathcal{R}_W < 1$, and unstable whenever $\mathcal{R}_W > 1$. Since the stunting subsystem admits a locally stable positive equilibrium s^*, the local invasion dynamics are governed by the wasting subsystem linearization. This completes the proof. □

The quantity $\mathcal{R}_W$ captures the progression potential of wasting in the presence of persistent background stunting prevalence. Since $s^* > 0$, chronic growth failure amplifies the transition from normal nutritional status to wasting through the interaction term $(1+\eta s^*)$. Consequently, populations with persistent stunting prevalence exhibit greater vulnerability to acute undernutrition dynamics.

3.5. Global Stability of the Wasting-Free Equilibrium

Let

$$b_1 = \mu+\delta+\phi_W, \qquad b_2 = \mu+\delta+\phi_{SW}.$$

The wasting progression threshold around the wasting-free equilibrium E_W is

$$\mathcal{R}_W = \frac{\gamma_{NW}(1+\eta s^*)(1-q_W)}{b_1},$$

where

$$s^* = \frac{\lambda_0}{\lambda_0+\phi_S+\mu+\delta}.$$

Theorem 3.5. *Assume $\mathcal{R}_W < 1$. Then the wasting-free equilibrium*

$$E_W = (o^*, n^*, 0, 0, s^*)$$

given in (22) is globally asymptotically stable in the feasible region

$$\Omega = \left\{ (o,n,w,sw,s) \in \mathbb{R}^5_+ : \; o+n+w+sw = 1, \; 0 \le s \le 1 \right\}.$$

In particular,

$$w(t),\, sw(t) \to 0 \qquad \text{as } t \to \infty.$$

Proof

Consider the Lyapunov function

$$V(w, sw) = w + sw,$$

which is nonnegative in Ω and satisfies

$$V = 0 \iff w = sw = 0.$$

Differentiating along solutions yields

$$\dot{V} = \frac{dw}{dt} + \frac{dsw}{dt}.$$

Using the model equations gives

$$\dot{V} = \gamma_{NW}(1 + \eta s)n - b_1 w - b_2 sw.$$

Since

$$0 \le s \le 1, \qquad n \le 1 - q_W,$$

we obtain

$$\dot{V} \le \gamma_{NW}(1 + \eta s^*)(1 - q_W) - b_1 w - b_2 sw.$$

Using

$$\mathcal{R}_W = \frac{\gamma_{NW}(1 + \eta s^*)(1 - q_W)}{b_1},$$

we write

$$\gamma_{NW}(1 + \eta s^*)(1 - q_W) = b_1 \mathcal{R}_W.$$

Hence,

$$\dot{V} \le b_1 \mathcal{R}_W - b_1 w - b_2 sw.$$

When

$$\mathcal{R}_W < 1,$$

the recovery and demographic removal processes dominate wasting progression, preventing persistence of acute undernutrition.

Moreover, the largest invariant set contained in

$$\{\dot{V} = 0\}$$

is

$$w = sw = 0.$$

Therefore, by LaSalle's invariance principle,

$$w(t),\, sw(t) \to 0 \qquad \text{as } t \to \infty.$$

Substituting

$$w(t),\, sw(t) \to 0$$

into the stunting subsystem yields

$$\frac{ds}{dt} = \lambda_0(1 - s) - (\phi_S + \mu + \delta)s,$$

whose equilibrium solution is

$$s^* = \frac{\lambda_0}{\lambda_0 + \phi_S + \mu + \delta}.$$

Consequently,

$$(o, n, w, sw, s) \to E_W,$$

and the wasting-free equilibrium is globally asymptotically stable. □

3.6. Summary of Analytical Results

The proposed wasting–stunting model admits a positively invariant and bounded feasible region, ensuring that all state variables remain biologically meaningful for nonnegative initial conditions. Consequently, the system is mathematically well posed and epidemiologically interpretable within the under-five population domain. The analytical results demonstrate that the wasting subsystem governs the principal threshold structure of the model through the wasting progression threshold $\mathcal{R}_W$. The model admits a biologically meaningful wasting-free equilibrium E_W, whose stability depends on the balance between wasting progression, recovery, demographic turnover, and chronic undernutrition amplification effects.

Local and global stability analyses show that when $\mathcal{R}_W < 1$, acute undernutrition cannot persist asymptotically, and the system converges toward the wasting-free equilibrium. Conversely, when $\mathcal{R}_W > 1$, persistent wasting dynamics emerge and generate sustained endemic acute malnutrition prevalence. Unlike the wasting subsystem, the stunting subsystem does not admit a biologically meaningful stunting-free equilibrium whenever $\lambda_0 > 0$. Consequently, chronic undernutrition persists at a positive endemic level even in the absence of wasting transmission. Persistent wasting prevalence further amplifies chronic undernutrition through the nonlinear interaction mechanism governed by the parameter α.

Overall, the analytical results reveal a hierarchical interaction structure in which wasting dynamics determine the principal epidemiological threshold behavior of the system, while chronic undernutrition persistence is regulated jointly by baseline chronic progression and wasting-induced amplification effects. These findings provide a theoretical foundation for the subsequent sensitivity analysis, numerical simulations, and long-term intervention projections.

4. Data Sources and Parameter Estimation

4.1. Available data sources

This study utilizes national prevalence data describing the nutritional status of children under five years of age in Indonesia during the period 2013–2024. The available observations include annual prevalence of wasting, severe wasting, and stunting at the population level. Additional demographic information, including infant population proportion and low birth weight prevalence, was obtained from *Profil Kesehatan Indonesia*, *Riskesdas*, and *SSGI* reports published during 2013–2025 [19, 21, 22, 41, 42, 43, 44, 45, 46, 47, 49].

National intervention coverage information related to nutritional rehabilitation programs was additionally obtained from the SIGIZI nutritional dashboard [50]. Since the available observations consist primarily of aggregate annual prevalence data, individual longitudinal nutritional transitions between compartments are not directly observable.

4.2. Data preprocessing and model inputs

Several preprocessing procedures were performed to ensure demographic consistency and temporal continuity of the model inputs. Low birth weight prevalence data for 2016 and 2017 were unavailable and were estimated using linear interpolation:

$$q_W(2016) \approx 0.070, \qquad q_W(2017) \approx 0.055.$$

4.3. Demographic parameter determination

The aging-out rate from the under-five population was structurally defined as

$$\delta = \frac{1}{5} = 0.2 \quad \text{year}^{-1}.$$

The natural mortality rate was estimated from national demographic statistics reported in *Profil Kesehatan Indonesia* [19]:

$$\mu = 0.00097 \quad \text{year}^{-1}.$$

Accordingly, the total demographic turnover rate was assumed constant:

$$\Lambda = \mu + \delta = 0.20097 \quad \text{year}^{-1}.$$

The time-varying low birth weight prevalence $q_W(t)$, obtained from national nutritional surveys and health reports [19, 21, 22, 41, 42, 43, 44, 45, 46, 47, 49], was used to partition the recruitment process into elevated-risk and normal-risk inflows:

$$\Lambda_W(t) = q_W(t)\Lambda, \qquad \Lambda_N(t) = (1 - q_W(t))\Lambda.$$

Thus, the total recruitment intensity remains constant over time, while the proportion entering the elevated wasting-risk pathway varies according to the observed low birth weight prevalence.

4.4. Semi-mechanistic parameter specification

Because the available datasets consist primarily of aggregate national prevalence observations rather than individual longitudinal nutritional trajectories, several biological transition parameters could not be directly inferred through classical transition-based estimation.

Therefore, recovery-related and interaction-related parameters were specified using a semi-mechanistic framework combining national nutritional statistics, published intervention evidence, epidemiological findings, and biologically informed assumptions.

The wasting recovery intensity ϕ_W was approximated using national nutritional improvement outcomes reported in the SIGIZI nutritional dashboard [50]. Under the Poisson transition assumption, the effective recovery intensity was represented as

$$\phi_W = -\ln(1 - r_W),$$

where r_W denotes the reported national proportion of nutritional improvement among children receiving intervention.

Because direct nationwide recovery observations for severe wasting were limited, the severe wasting recovery intensity was specified using a proportional scaling formulation:

$$\phi_{SW} = c\,\phi_W, \qquad 0 < c < 1,$$

where c denotes a proportional recovery scaling coefficient reflecting the slower recovery dynamics associated with severe wasting conditions.

For stunting recovery, direct nationwide recovery observations were unavailable. Consequently, the effective stunting recovery intensity was approximated by combining national intervention coverage information from the SIGIZI dashboard with published nutritional rehabilitation effectiveness reported in Indonesian clinical intervention studies [50, 51].

Let r_{ref} denote the proportion of stunting cases receiving nutritional intervention referral services, and let r_{eff} denote the reported intervention effectiveness among treated children. The effective population-level stunting recovery intensity was then approximated as

$$\phi_S = r_{\text{ref}}\, r_{\text{eff}}.$$

This quantity should be interpreted as an effective population-level chronic recovery intensity rather than a direct clinical recovery probability.

Interaction parameters governing the bidirectional relationship between wasting and stunting were specified using epidemiological evidence reported in previous nutritional studies [16].

The parameter α represents wasting-induced amplification of chronic growth failure, whereas η denotes increased wasting susceptibility associated with chronic undernutrition.

Together, these quantities characterize the mutual reinforcement mechanism linking acute and chronic undernutrition within the proposed coupled dynamical system.

4.5. Calibration framework

The dominant progression-related parameters were estimated through nonlinear least-squares calibration against the observed prevalence trajectories for wasting, severe wasting, and stunting.

The calibrated parameters were

$$\gamma_{NW}, \qquad \gamma_{WS}, \qquad \lambda_0,$$

where:

- γ_{NW} denotes the progression intensity from normal nutritional status to wasting;
- γ_{WS} represents the progression intensity from wasting to severe wasting;
- λ_0 corresponds to the baseline chronic stunting progression intensity.

The objective function was defined as

$$J(\Theta) = \sum_{i=1}^{n} \left[(W_i^{\text{model}} - W_i^{\text{data}})^2 + (SW_i^{\text{model}} - SW_i^{\text{data}})^2 + (S_i^{\text{model}} - S_i^{\text{data}})^2 \right],$$

where Θ denotes the calibrated parameter vector and n the number of observational time points.

Parameter optimization was performed numerically using constrained nonlinear least-squares minimization, while the governing differential equation system was numerically integrated during optimization to generate simulated prevalence trajectories.

To evaluate practical parameter identifiability, profile likelihood analysis was performed for the principal calibrated parameters.

For each parameter θ_i, the profile likelihood was defined as

$$PL(\theta_i) = \min_{\Theta \setminus \theta_i} J(\Theta),$$

where $J(\Theta)$ denotes the calibration objective function.

Bootstrap resampling was additionally performed to quantify parameter uncertainty and construct approximate confidence intervals for the calibrated parameters.

Overall, the resulting framework combines mechanistic nutritional dynamics with data-driven calibration while preserving biological interpretability under partial observability constraints.

5. Results

5.1. Motivation for semi-mechanistic parameter specification

The available nutritional observations in this study consist primarily of aggregate annual prevalence data for wasting, severe wasting, and stunting at the national level. Consequently, individual longitudinal nutritional transitions between compartments are not directly observable. Under such conditions, simultaneous unconstrained estimation of all biological transition parameters may produce weakly constrained recovery dynamics and biologically unrealistic parameter combinations, particularly for processes that are only indirectly reflected through aggregate prevalence trajectories.

In particular, recovery-related mechanisms are substantially more difficult to infer from population-level prevalence observations alone because aggregate prevalence dynamics primarily contain information regarding dominant progression processes rather than individual rehabilitation behavior. Furthermore, severe wasting prevalence remained comparatively small and exhibited limited temporal variability during the observational period, reducing the information available for reliably estimating downstream deterioration and recovery processes.

These limitations motivate the use of a semi-mechanistic parameter specification framework in which recovery-related and interaction-related parameters are informed using external intervention evidence, epidemiological findings, and biologically informed assumptions, while the dominant progression-related parameters are estimated directly from the observed prevalence trajectories. This strategy preserves biological interpretability while reducing overparameterization and improving practical identifiability under partial observability constraints.

5.2. Semi-mechanistic parameter estimation

Using the semi-mechanistic framework described in Section 4, recovery-related and interaction-related parameters were approximated using national nutritional statistics, intervention evidence, epidemiological findings, and biologically informed assumptions.

For wasting recovery, the national nutritional improvement proportion obtained from the SIGIZI nutritional dashboard produced an estimated effective recovery intensity

$$\phi_W \approx 0.190.$$

Because direct nationwide recovery observations for severe wasting were limited, the severe wasting recovery intensity was specified using proportional scaling relative to wasting recovery:

$$\phi_{SW} = 0.5\,\phi_W,$$

yielding

$$\phi_{SW} \approx 0.095.$$

This result reflects the expected slower recovery dynamics associated with severe wasting conditions relative to moderate wasting.

For stunting recovery, the effective recovery intensity was approximated by combining national referral coverage information from the SIGIZI dashboard with published nutritional rehabilitation effectiveness reported in Indonesian clinical intervention studies.

Using the national referral coverage

$$r_{\text{ref}} = 0.0058$$

together with the reported rehabilitation effectiveness

$$r_{\text{eff}} = \frac{166}{381} \approx 0.436,$$

the resulting effective population-level stunting recovery intensity was obtained as

$$\phi_S = r_{\text{ref}} r_{\text{eff}} \approx 0.0025.$$

This relatively small value indicates that population-level recovery from chronic undernutrition occurs substantially more slowly than short-term therapeutic improvement observed in controlled clinical intervention settings.

Interaction parameters governing the wasting–stunting coupling mechanism were specified using epidemiological evidence reported in previous nutritional studies [16].

The wasting-induced stunting amplification coefficient was initialized as

$$\alpha = 0.8,$$

reflecting the substantially elevated risk of concurrent wasting–stunting outcomes among undernourished children.

Meanwhile, the parameter

$$\eta = 0.5$$

was adopted to represent moderate amplification of wasting susceptibility in the presence of chronic undernutrition.

Together, these parameter estimates characterize the bidirectional reinforcement mechanism linking acute and chronic undernutrition within the proposed dynamical system.

5.3. Calibration results and practical identifiability analysis

Under the semi-mechanistic framework, demographic quantities, recovery-related parameters, and interaction coefficients were specified externally using nutritional statistics and epidemiological evidence. Consequently, the calibration procedure focused primarily on the dominant progression-related parameters $\gamma_{NW}, \gamma_{WS}, \lambda_0$.

The resulting calibrated parameter estimates were obtained as

$$\gamma_{NW} = 0.0219, \qquad \gamma_{WS} = 0.0178, \qquad \lambda_0 = 0.0442.$$

Table 2 summarizes the final parameter values, estimation strategies, and data sources used in the calibrated wasting–stunting model.

Table 2. Final parameter values, estimation strategies, and data sources used in the calibrated wasting–stunting model.

Symbol	**Value**	**Method**	**Source**
Demographic parameters			
μ	0.00097	Computed from national mortality statistics	[19]
δ	0.20	Structural aging-out assumption	–
Λ	0.20097	Normalized recruitment balance ($\Lambda = \mu + \delta$)	Derived
Time-varying model input			
$q_W(t)$	0.033–0.102	Interpolated annual low birth weight prevalence	[41, 42, 43, 44, 45, 19, 47, 48, 49]
Recovery-related parameters			
ϕ_W	0.190	National PMT recovery approximation	[50]
ϕ_{SW}	0.095	Semi-mechanistic proportional scaling	Derived
ϕ_S	0.0025	Population-level intervention recovery approximation based on SIGIZI referral coverage and nutritional rehabilitation effectiveness	[50, 51]
Interaction parameters			
η	0.5	Moderate chronic amplification assumption	[16]
α	0.8	Literature-informed interaction initialization	[16]
Calibrated progression parameters			
γ_{NW}	0.0219	Semi-mechanistic calibration	This study
γ_{WS}	0.0178	Semi-mechanistic calibration	This study
λ_0	0.0442	Semi-mechanistic calibration	This study

Bootstrap estimation produced the following approximate 95% confidence intervals $\gamma_{NW} \in (0.0204, 0.0249), \gamma_{WS} \in (0.0068, 0.0640)$, and $\lambda_0 \in (0.0421, 0.0538)$. The comparatively wider confidence interval obtained for γ_{WS} indicates weaker practical identifiability for severe wasting progression dynamics relative to the principal wasting and chronic progression parameters. Figure 1 compares the simulated prevalence trajectories against the observed national prevalence data for wasting, severe wasting, and stunting during 2017–2024.

The calibrated model successfully reproduces the dominant nutritional trajectories observed in the national prevalence data. In particular, the model captures the declining trend in stunting prevalence during 2017–2024

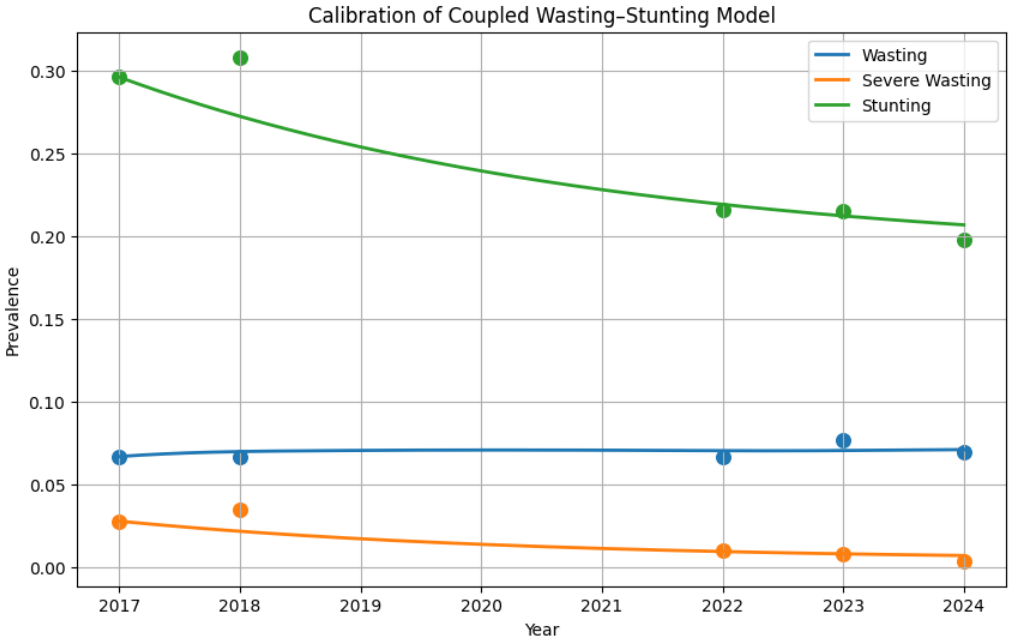

Figure 1. Calibration results for wasting, severe wasting, and stunting prevalence during 2017–2024. Solid curves represent simulated model trajectories, whereas markers denote observed national prevalence data.

together with the relatively stable wasting prevalence observed at the national level. For wasting prevalence, the simulated trajectory remains relatively stable and follows the general magnitude of the observed national prevalence levels. Similarly, the model reproduces the declining trend observed for severe wasting prevalence, although short-term fluctuations in the empirical observations are not fully captured due to the aggregate deterministic structure of the model. Importantly, the calibrated stunting dynamics remain biologically consistent with the slow and cumulative nature of chronic growth failure. The relatively small estimated value of ϕ_S suggests that effective population-level recovery from chronic undernutrition occurs substantially more slowly than individual therapeutic improvement observed under intensive clinical intervention settings. These findings indicate that aggregate national stunting prevalence is governed primarily by long-term structural nutritional dynamics rather than rapid short-term recovery processes alone.

To evaluate practical parameter identifiability, profile likelihood analysis was subsequently performed for the principal calibrated progression parameters. For a parameter θ_i, the profile likelihood was defined as

$$PL(\theta_i) = \min_{\Theta \setminus \theta_i} J(\Theta),$$

where $J(\Theta)$ denotes the calibration objective function.

Figure 2 presents the resulting profile likelihood trajectories for the dominant progression parameters. The profile likelihood analysis demonstrated that the principal progression parameters remained practically identifiable under the available aggregate prevalence observations. In particular, both γ_{NW} and λ_0 exhibited well-defined convex likelihood structures with clear minima, indicating stable parameter estimation. In contrast, the likelihood profile for γ_{WS} appeared substantially flatter, suggesting weaker practical identifiability for severe wasting progression dynamics. This behavior is likely attributable to the relatively small magnitude and limited variability of severe wasting prevalence observations at the national level.

The estimated profile likelihood spreads were obtained as $\gamma_{NW} : 0.02304$, $\gamma_{WS} : 0.00045$, $\lambda_0 : 0.02694$. These findings indicate that aggregate national prevalence observations primarily contain information regarding the dominant progression dynamics of the nutritional system, whereas downstream deterioration

processes associated with severe wasting remain only partially constrained under population-level surveillance observations.

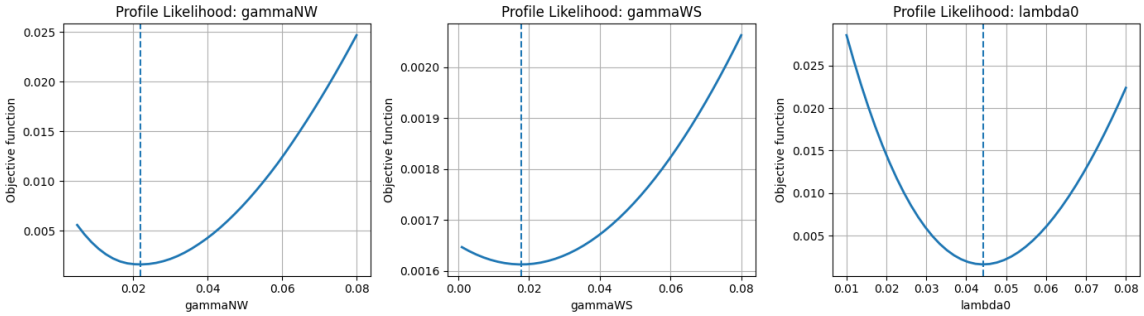

Figure 2. Profile likelihood trajectories for the principal calibrated progression parameters. Well-defined convex profiles indicate practical identifiability under aggregate national prevalence observations.

The minimum objective function value obtained during calibration was $J_{\min} = 0.00161$, indicating satisfactory agreement between the simulated trajectories and the aggregate national prevalence observations. Overall, the calibration and identifiability analyses demonstrate that the proposed framework provides a biologically interpretable and data-consistent representation of coupled wasting–stunting dynamics while remaining sufficiently parsimonious for long-term population-level nutritional analysis under partial observability constraints.

5.4. Local Sensitivity Analysis

To evaluate the influence of model parameters on the wasting–stunting dynamics, a local normalized sensitivity analysis was performed using the final semi-mechanistically recalibrated parameter set. Each parameter was independently perturbed by 10% around its calibrated baseline value while all remaining parameters were held fixed. The normalized local sensitivity index was computed numerically as

$$S_p = \frac{\Delta Y / Y}{\Delta p / p},$$

where Y denotes the corresponding model output and p represents the perturbed parameter. The analysis was conducted separately for wasting prevalence, severe wasting prevalence, and stunting prevalence during 2017–2024.

5.4.1. Sensitivity structure of wasting dynamics The wasting compartment exhibited a sensitivity structure dominated primarily by wasting incidence and wasting recovery mechanisms. Among all parameters, the transition parameter γ_{NW} generated the largest sensitivity magnitude, followed by the recovery parameter ϕ_W. These findings indicate that wasting prevalence is governed mainly by the balance between nutritional deterioration from the normal state and subsequent recovery from wasting conditions.

The temporal sensitivity trajectories in Figure 3 show that the sensitivity associated with γ_{NW} increases monotonically throughout the simulation period and reaches the highest final-year magnitude among all wasting-related parameters. This behavior indicates that wasting prevalence is sustained primarily through continuous nutritional deterioration from the normal nutritional compartment into wasting conditions.

The wasting recovery parameter ϕ_W generated the second-largest sensitivity magnitude and exhibited consistently negative trajectories throughout the simulation period. This confirms the stabilizing role of wasting recovery interventions in suppressing acute malnutrition prevalence. However, the larger magnitude associated with γ_{NW} suggests that prevention of wasting incidence may produce greater long-term impact than recovery interventions alone.

The parameter η, representing increased wasting susceptibility in the presence of chronic undernutrition, generated moderate positive sensitivity values. This finding indicates the existence of a secondary feedback

Table 3. Local sensitivity ranking for wasting prevalence.

No.	Parameter	Mean	Maximum	Final-Year
1	γ_{NW}	0.4705	0.6387	0.6387
2	ϕ_W	0.2960	0.4078	0.4078
3	η	0.0518	0.0656	0.0631
4	γ_{WS}	0.0297	0.0424	0.0424
5	λ_0	0.0135	0.0292	0.0292
6	α	0.0009	0.0018	0.0018
7	ϕ_{SW}	0.0008	0.0035	0.0025
8	ϕ_S	0.0002	0.0005	0.0005

pathway through which chronic undernutrition amplifies wasting vulnerability, although the magnitude remains substantially smaller than the direct wasting incidence pathway governed by γ_{NW}.

In contrast, the parameters α, ϕ_{SW}, and ϕ_S produced extremely small sensitivity magnitudes for wasting prevalence. These results indicate that downstream severe wasting recovery and chronic stunting recovery exert minimal direct influence on the overall wasting burden within the present coupled framework.

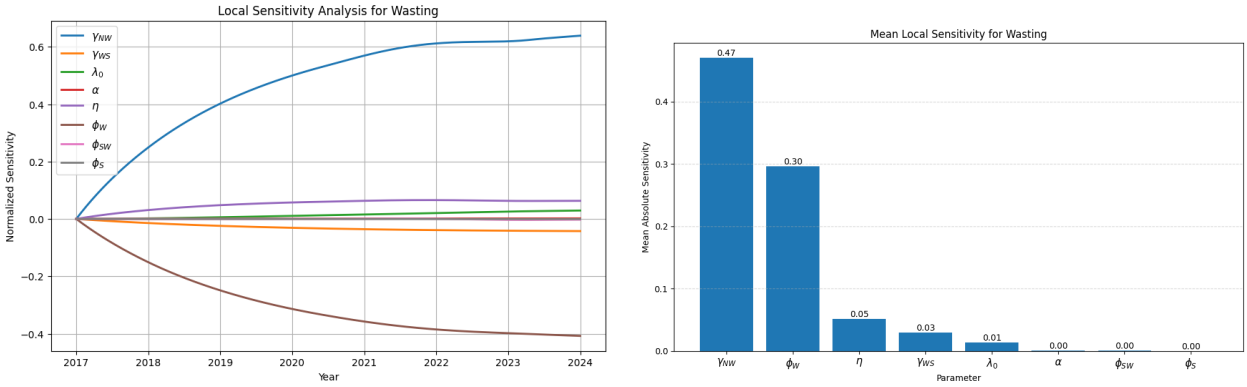

Figure 3. Local sensitivity analysis results for wasting prevalence: (a) temporal local sensitivity trajectories and (b) average local sensitivity ranking.

The temporal sensitivity trajectories further demonstrate a clear asymmetry between deterioration and recovery mechanisms. Parameters associated with nutritional deterioration produce positive sensitivity trajectories, whereas recovery-related parameters generate negative trajectories, confirming their opposing epidemiological roles in acute malnutrition regulation.

Meanwhile, the average sensitivity ranking in Figure 3 highlights the dominant contribution of wasting incidence and wasting recovery to overall wasting prevalence. The substantially larger average sensitivity magnitudes associated with γ_{NW} and ϕ_W indicate that interventions focused on preventing early wasting deterioration and strengthening nutritional recovery are likely to generate the greatest reduction in population-level wasting prevalence.

5.4.2. Sensitivity structure of severe wasting dynamics The severe wasting compartment exhibited a sensitivity structure dominated primarily by progression and recovery mechanisms associated with severe acute malnutrition. In particular, the severe wasting recovery parameter ϕ_{SW} generated the largest average sensitivity magnitude, followed by the progression parameter γ_{WS} and the upstream wasting incidence parameter γ_{NW}.

Table 4. Local sensitivity ranking for severe wasting prevalence.

No.	Parameter	Mean	Maximum	Final-Year
1	ϕ_{SW}	0.2626	0.4329	0.4329
2	γ_{WS}	0.2193	0.4824	0.4824
3	γ_{NW}	0.1008	0.2754	0.2754
4	ϕ_W	0.0631	0.1745	0.1745
5	η	0.0113	0.0294	0.0294
6	λ_0	0.0025	0.0093	0.0093
7	α	0.0002	0.0006	0.0006
8	ϕ_S	0.0000	0.0002	0.0002

The temporal sensitivity trajectories in Figure 4 reveal a hierarchical deterioration cascade $N \to W \to SW$, in which increases in wasting incidence eventually propagate into severe wasting prevalence through cumulative progression dynamics.

The progression parameter γ_{WS} generated the largest final-year sensitivity magnitude, indicating that transitions from wasting toward severe wasting constitute the principal mechanism sustaining severe acute malnutrition prevalence.

Meanwhile, the severe wasting recovery parameter ϕ_{SW} exhibited consistently negative sensitivity trajectories throughout the simulation period. This confirms the epidemiological importance of therapeutic recovery interventions in reducing severe wasting burden.

The wasting recovery parameter ϕ_W also generated negative sensitivity values, suggesting that improvements in recovery during earlier wasting stages indirectly suppress downstream severe wasting accumulation by interrupting deterioration pathways before children transition into more critical nutritional states.

In contrast, parameters associated primarily with chronic undernutrition dynamics, including α, λ_0, and ϕ_S, produced extremely small sensitivity magnitudes. These results indicate that severe wasting prevalence is governed predominantly by acute deterioration pathways rather than chronic stunting progression mechanisms.

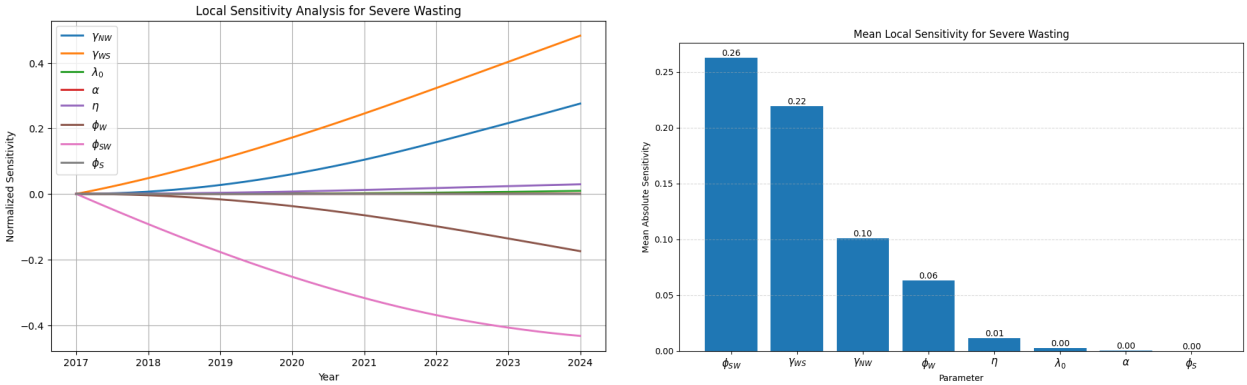

Figure 4. Local sensitivity analysis results for severe wasting prevalence: (a) temporal local sensitivity trajectories and (b) average local sensitivity ranking.

The temporal sensitivity trajectories further demonstrate a pronounced divergence between progression and recovery effects over time. Parameters associated with deterioration mechanisms generate positive trajectories, whereas recovery-related parameters generate negative trajectories, confirming their opposing influences on severe acute malnutrition burden.

Overall, the average sensitivity ranking in Figure 4 highlights the dominant contribution of deterioration and recovery mechanisms directly associated with severe wasting progression. These findings indicate that interventions aimed at interrupting progression toward severe wasting and strengthening therapeutic recovery are likely to generate the greatest reduction in severe acute malnutrition prevalence.

5.4.3. Sensitivity structure of stunting dynamics The sensitivity analysis revealed that stunting prevalence is governed predominantly by baseline chronic progression dynamics rather than by wasting-related interaction mechanisms. Among all parameters, the baseline stunting progression parameter λ_0 generated the largest sensitivity magnitude by a substantial margin, followed by the interaction parameter α and the wasting incidence parameter γ_{NW}.

Table 5. Local sensitivity ranking for stunting prevalence.

No.	Parameter	Mean	Maximum	Final-Year
1	λ_0	0.3279	0.5744	0.5744
2	α	0.0210	0.0346	0.0346
3	γ_{NW}	0.0074	0.0166	0.0166
4	ϕ_S	0.0058	0.0091	0.0091
5	ϕ_W	0.0046	0.0105	0.0105
6	η	0.0008	0.0018	0.0018
7	ϕ_{SW}	0.0007	0.0014	0.0014
8	γ_{WS}	0.0001	0.0002	0.0002

The dominant sensitivity associated with λ_0 indicates that long-term stunting prevalence is regulated primarily by structural chronic growth-failure mechanisms rather than by short-term acute malnutrition fluctuations alone.

As shown in Figure 5, the sensitivity trajectory corresponding to λ_0 increases progressively throughout the simulation period and reaches substantially larger magnitudes than all other parameters. This behavior reflects the cumulative and slow-moving nature of chronic undernutrition dynamics at the population level.

The interaction parameter α generated positive but comparatively small sensitivity values, confirming that wasting contributes to chronic growth failure through the coupled wasting–stunting amplification mechanism incorporated into the model structure. However, the substantially smaller magnitude relative to λ_0 indicates that wasting acts primarily as a secondary amplification pathway rather than the principal driver of long-term stunting persistence.

Similarly, the wasting incidence parameter γ_{NW} produced relatively small positive sensitivity values, indicating that increases in wasting prevalence indirectly propagate into chronic undernutrition burden through the interaction structure of the model.

In contrast, the progression parameter γ_{WS} and the severe wasting recovery parameter ϕ_{SW} generated extremely weak sensitivity magnitudes for stunting prevalence. These findings indicate that downstream severe wasting dynamics exert only minimal direct influence on long-term chronic growth failure within the present coupled framework.

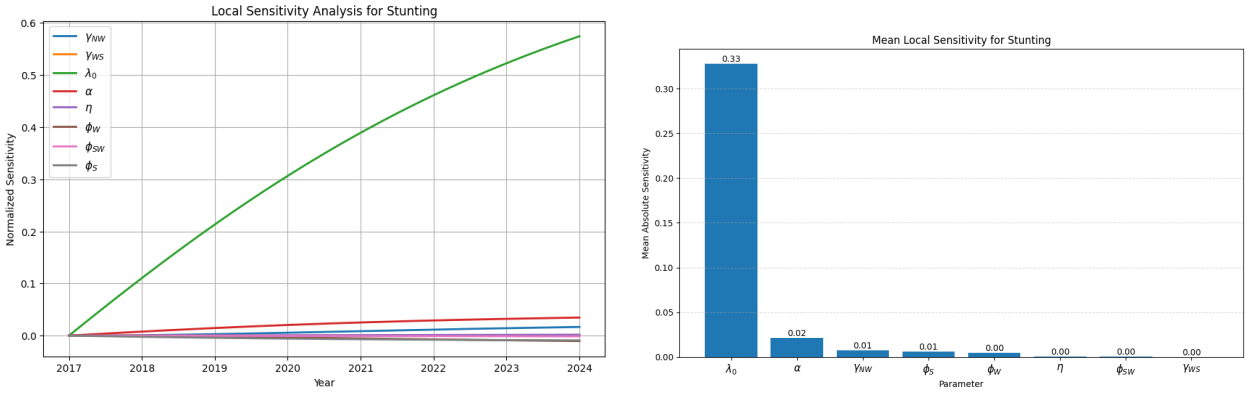

Figure 5. Local sensitivity analysis results for stunting prevalence: (a) temporal local sensitivity trajectories and (b) average local sensitivity ranking.

The temporal sensitivity trajectories further demonstrate a strong asymmetry between structural chronic progression mechanisms and wasting-induced amplification effects. Parameters associated with chronic deterioration processes generate positive trajectories, whereas recovery-related parameters generate comparatively weak suppressive effects due to the very small effective population-level chronic recovery intensity incorporated into the model.

Overall, the average sensitivity ranking in Figure 5 confirms that long-term stunting persistence is governed primarily by baseline chronic nutritional dynamics, while wasting-related mechanisms contribute mainly as secondary amplification pathways. These findings support the theoretical results indicating that chronic undernutrition persistence emerges predominantly through structural long-term progression processes rather than rapid short-term nutritional fluctuations.

5.4.4. Overall biological interpretation Overall, the local sensitivity analysis demonstrates that the proposed wasting–stunting system possesses highly compartment-specific regulatory structures, indicating that each nutritional state is governed by distinct dominant biological mechanisms.

Wasting prevalence is controlled primarily by the balance between wasting incidence and wasting recovery, whereas severe wasting prevalence is governed mainly by progression and therapeutic recovery within the severe acute malnutrition pathway. In contrast, stunting prevalence is regulated predominantly by baseline chronic progression dynamics, with wasting-related mechanisms contributing mainly through secondary amplification effects. These findings reveal the existence of a hierarchical coupling structure within the proposed system. Early nutritional deterioration occurring in the wasting compartment propagates downstream into severe wasting accumulation and simultaneously contributes indirectly to chronic growth impairment through the wasting–stunting interaction mechanism. However, the substantially smaller sensitivity magnitudes associated with wasting-related parameters in the stunting subsystem indicate that chronic undernutrition persistence is driven primarily by long-term structural nutritional dynamics rather than by acute malnutrition processes alone.

From an epidemiological perspective, the sensitivity structure suggests that interventions targeting early wasting prevention and recovery are likely to produce the greatest reductions in acute malnutrition prevalence, whereas sustained long-term reduction of stunting prevalence requires broader structural improvements addressing chronic growth-failure dynamics at the population level. Collectively, these findings support the biological consistency of the proposed coupled wasting–stunting model and demonstrate that acute and chronic undernutrition exhibit asymmetric but interconnected population-level dynamics within the proposed framework.

5.5. Sensitivity analysis of the wasting progression threshold

To further investigate the dominant mechanisms governing wasting persistence, normalized local sensitivity analysis was performed for the wasting progression threshold

$$\mathcal{R}_W = \frac{\gamma_{NW}(1+\eta s^*)(1-q_W)}{\mu+\delta+\phi_W}.$$

Using the final calibrated parameter values together with the equilibrium stunting level s^*, the threshold quantity was obtained as $\mathcal{R}_W = 0.059282$. This threshold value remains substantially below unity, indicating that the calibrated nutritional system lies within a subcritical wasting regime. Biologically, this result implies that acute malnutrition cannot maintain self-sustaining long-term persistence under the present parameter configuration.

The normalized sensitivity indices for $\mathcal{R}_W$ are summarized in Table 6.

Table 6. Normalized sensitivity indices for $\mathcal{R}_W$.

Parameter	Sensitivity Index	Absolute Value
γ_{NW}	1.000000	1.000000
ϕ_W	−0.485968	0.485968
η	0.090082	0.090082
s^*	0.090082	0.090082
q_W	−0.038422	0.038422

The wasting progression parameter γ_{NW} generated the largest positive sensitivity index, indicating that wasting persistence is governed primarily by the deterioration process from the normal nutritional compartment into wasting conditions. Quantitatively, a 1% increase in γ_{NW} produces an approximately proportional 1% increase in $\mathcal{R}_W$, demonstrating the dominant structural role of wasting incidence in controlling threshold behavior.

Overall, the sensitivity structure indicates that wasting persistence is regulated primarily by the balance between nutritional deterioration and recovery processes, with deterioration dynamics exerting the dominant positive influence. In epidemiological terms, the persistence potential of wasting depends more strongly on the rate at which nutritionally vulnerable children deteriorate into wasting conditions than on downstream severe wasting progression mechanisms. Consequently, prevention of early nutritional decline constitutes a principal mechanism for maintaining the wasting threshold below unity.

In contrast, the wasting recovery parameter ϕ_W generated a comparatively large negative sensitivity index. This confirms the stabilizing role of nutritional rehabilitation and recovery interventions in suppressing wasting persistence. The relatively large magnitude associated with ϕ_W further indicates that strengthening wasting recovery substantially reduces the effective persistence capacity of acute malnutrition within the population.

The negative sign associated with ϕ_W additionally reflects an important biological asymmetry within the wasting subsystem: deterioration processes amplify persistence, whereas recovery processes suppress long-term transmission potential. This antagonistic balance forms the principal regulatory structure governing wasting dynamics.

Meanwhile, the interaction parameter η and the equilibrium stunting level s^* generated identical positive sensitivity indices, reflecting the multiplicative interaction structure $(1+\eta s^*)$ embedded in the threshold formulation. Biologically, this result demonstrates that chronic undernutrition amplifies wasting persistence through increased nutritional vulnerability associated with persistent stunting prevalence.

Nevertheless, the sensitivity magnitudes associated with η and s^* remained substantially smaller than those associated with γ_{NW} and ϕ_W. This indicates that chronic undernutrition acts primarily as a secondary amplification pathway rather than the dominant driver of wasting persistence.

The low birth weight recruitment parameter q_W generated only a relatively small sensitivity magnitude. Although low birth weight contributes to nutritional vulnerability through recruitment inflow mechanisms, its comparatively

weak sensitivity indicates that long-term wasting persistence is influenced more strongly by postnatal nutritional deterioration and recovery processes than by baseline recruitment composition alone.

Figure 6 illustrates the normalized sensitivity structure of $\mathcal{R}_W$.

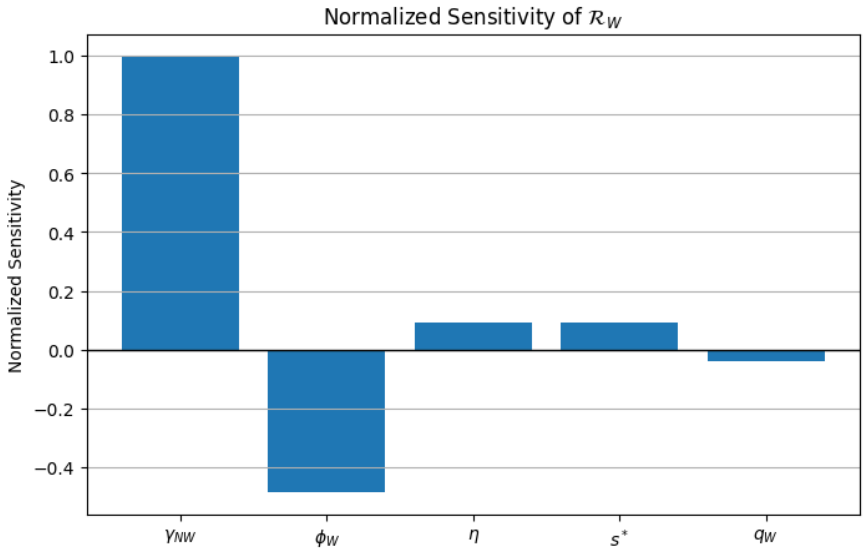

Figure 6. Normalized local sensitivity indices for the wasting progression threshold $\mathcal{R}_W$.

Overall, the threshold sensitivity analysis demonstrates that the proposed wasting–stunting system possesses a hierarchical regulatory structure in which wasting persistence is governed primarily by acute nutritional deterioration and recovery dynamics, while chronic undernutrition contributes indirectly through secondary amplification effects.

These findings remain consistent with the theoretical stability analysis, the global sensitivity analysis, and the calibrated numerical simulations. Collectively, the results indicate that the wasting subsystem acts as the principal dynamical regulator of the coupled nutritional system, whereas chronic undernutrition modifies long-term persistence through slower structural amplification mechanisms.

5.6. Global Sensitivity Analysis

To complement the local sensitivity analysis, a global sensitivity analysis was performed using variance-based Sobol sensitivity indices. Unlike local sensitivity methods, which evaluate small perturbations around a single calibrated parameter set, Sobol analysis quantifies the contribution of parameter uncertainty across the admissible parameter space while accounting for nonlinear effects and higher-order parameter interactions.

Let

$$Y = f(\mathbf{X})$$

denote a model output variable depending on the parameter vector

$$\mathbf{X} = (X_1, X_2, \ldots, X_k).$$

The Sobol first-order sensitivity index for parameter X_i is defined as

$$S_i = \frac{\mathrm{Var}_{X_i}\left(\mathbb{E}[Y \mid X_i]\right)}{\mathrm{Var}(Y)},$$

which measures the direct contribution of parameter X_i to the total output variance.

The total-order sensitivity index is given by

$$S_{T_i} = 1 - \frac{\mathrm{Var}_{\mathbf{X}_{\sim i}}\left(\mathbb{E}[Y \mid \mathbf{X}_{\sim i}]\right)}{\mathrm{Var}(Y)},$$

where $\mathbf{X}_{\sim i}$ denotes all parameters except X_i. The quantity S_{T_i} measures the total contribution of parameter X_i, including all higher-order interaction effects.

The Sobol analysis was performed using Saltelli sampling with 5120 total simulations over biologically plausible parameter ranges centered around the final calibrated parameter values. The final-year prevalence outputs for wasting, severe wasting, and stunting were used as target response variables.

5.6.1. Global sensitivity structure of wasting prevalence Table 7 and Figure 7 demonstrate that the global sensitivity structure of wasting prevalence is dominated primarily by the wasting progression parameter γ_{NW}, with

$$S_1 = 0.6854, \qquad S_T = 0.6896.$$

These indices indicate that nearly 70% of the total variance in wasting prevalence is directly attributable to uncertainty in the nutritional deterioration process from the normal nutritional compartment into wasting conditions.

The dominance of γ_{NW} is visually evident in Figure 7, where both the first-order and total-order Sobol bars corresponding to γ_{NW} substantially exceed those of all remaining parameters. Moreover, the very small difference between S_1 and S_T indicates that the influence of γ_{NW} arises predominantly through direct effects rather than higher-order nonlinear interactions.

The second-largest contribution was generated by the wasting recovery parameter ϕ_W,

$$S_1 = 0.3024, \qquad S_T = 0.3018.$$

This result confirms the important stabilizing role of wasting recovery interventions in regulating acute malnutrition prevalence. Biologically, the wasting subsystem is therefore governed primarily by the antagonistic balance between nutritional deterioration and nutritional recovery.

The interaction parameter η generated only a very small contribution,

$$S_1 = 0.0067,$$

indicating that chronic undernutrition contributes only weakly to uncertainty in wasting prevalence at the global population level. Similarly, the remaining parameters produced negligible Sobol indices, suggesting that downstream severe wasting progression and chronic stunting recovery exert minimal direct control over overall wasting dynamics.

Table 7. Sobol global sensitivity indices for wasting prevalence.

Parameter	S_1	S_T
γ_{NW}	0.6854	0.6896
ϕ_W	0.3024	0.3018
η	0.0067	0.0069
γ_{WS}	0.0022	0.0031
λ_0	0.0013	0.0015
ϕ_{SW}	0.0000	0.0000
α	0.0000	0.0000
ϕ_S	0.0000	0.0000

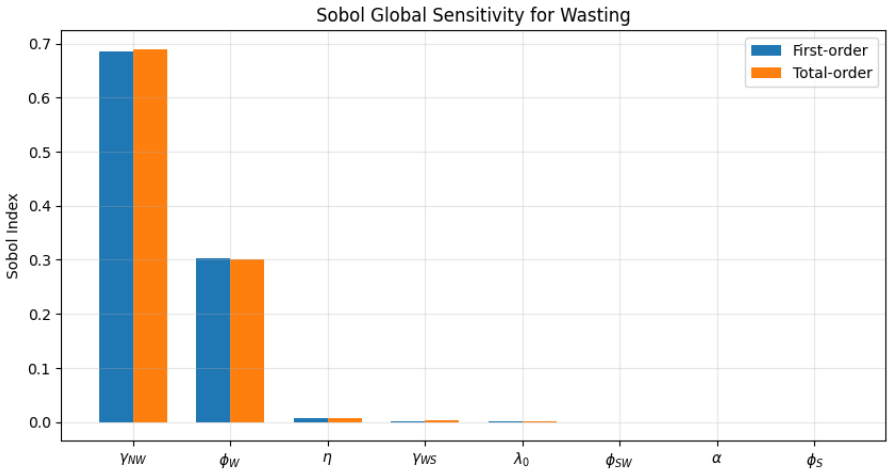

Figure 7. Sobol global sensitivity indices for wasting prevalence.

Overall, the global sensitivity structure reveals that wasting prevalence is governed overwhelmingly by direct acute nutritional deterioration and recovery mechanisms. The relatively weak contribution of chronic interaction parameters further suggests that wasting dynamics remain primarily controlled by acute nutritional processes rather than chronic undernutrition amplification effects.

5.6.2. Global sensitivity structure of severe wasting prevalence Table 8 and Figure 8 demonstrate that the global sensitivity structure of severe wasting prevalence is governed primarily by the progression parameter γ_{WS} and the severe wasting recovery parameter ϕ_{SW}.

The progression parameter γ_{WS} generated the largest Sobol contribution,

$$S_1 = 0.4330, \qquad S_T = 0.4336,$$

indicating that transitions from wasting toward severe wasting constitute the dominant mechanism controlling severe acute malnutrition prevalence.

The severe wasting recovery parameter ϕ_{SW} produced the second-largest contribution,

$$S_1 = 0.3634, \qquad S_T = 0.3650.$$

These findings indicate that severe wasting prevalence is regulated primarily by the balance between deterioration toward critical nutritional states and subsequent therapeutic recovery.

Biologically, this result reflects the hierarchical deterioration cascade

$$N \to W \to SW,$$

in which severe wasting emerges predominantly through cumulative worsening of existing wasting conditions.

The upstream wasting incidence parameter γ_{NW} generated a moderate contribution,

$$S_1 = 0.1403,$$

demonstrating that increases in wasting incidence indirectly propagate into severe wasting prevalence through downstream deterioration pathways.

Meanwhile, the wasting recovery parameter ϕ_W produced a comparatively smaller contribution,

$$S_1 = 0.0580,$$

indicating that recovery during earlier wasting stages indirectly suppresses severe wasting accumulation by interrupting progression pathways before children transition into critical nutritional states.

Table 8. Sobol global sensitivity indices for severe wasting prevalence.

Parameter	S_1	S_T
γ_{WS}	0.4330	0.4336
ϕ_{SW}	0.3634	0.3650
γ_{NW}	0.1403	0.1427
ϕ_W	0.0580	0.0604
η	0.0015	0.0016
λ_0	0.0004	0.0002
α	0.0000	0.0000
ϕ_S	0.0000	0.0000

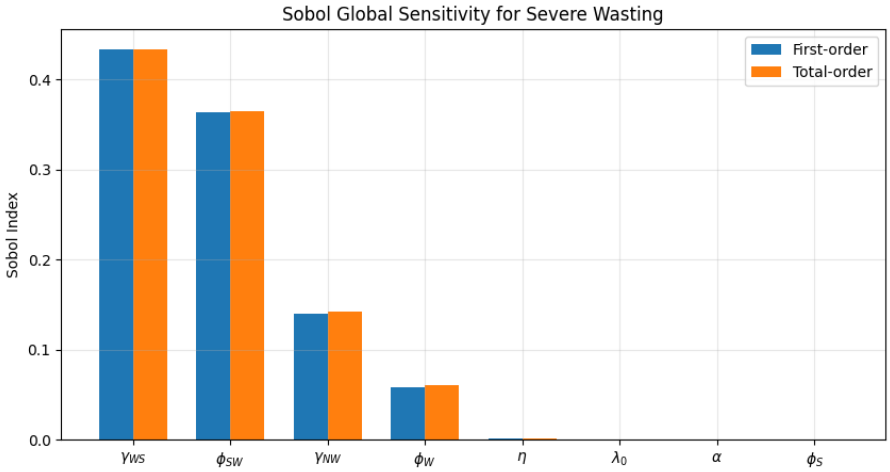

Figure 8. Sobol global sensitivity indices for severe wasting prevalence.

The very small gap between first-order and total-order indices across all parameters further indicates that severe wasting dynamics exhibit relatively weak higher-order nonlinear interactions. Consequently, uncertainty in severe wasting prevalence is governed mainly by a limited subset of dominant deterioration and recovery mechanisms.

Overall, the global sensitivity analysis demonstrates that severe wasting prevalence is regulated predominantly by direct progression and recovery dynamics associated with severe acute malnutrition rather than by chronic undernutrition amplification processes.

5.6.3. Global sensitivity structure of stunting prevalence Table 9 and Figure 9 demonstrate that the global sensitivity structure of stunting prevalence is overwhelmingly dominated by the baseline chronic progression parameter λ_0, which generated $S_1 = 0.9947, \quad S_T = 0.9951$. These Sobol indices indicate that nearly the entire variance in long-term stunting prevalence is explained directly by uncertainty in the baseline chronic progression process itself. In practical terms, the stunting subsystem behaves almost as a structurally autonomous chronic process whose long-term dynamics are governed primarily by intrinsic progression mechanisms rather than by short-term fluctuations in acute malnutrition compartments.

Table 9. Sobol global sensitivity indices for stunting prevalence.

Parameter	S_1	S_T
λ_0	0.9947	0.9951
α	0.0038	0.0036
γ_{NW}	0.0007	0.0008
ϕ_W	0.0003	0.0004
ϕ_S	0.0001	0.0002
η	0.0000	0.0000
ϕ_{SW}	0.0000	0.0000
γ_{WS}	0.0000	0.0000

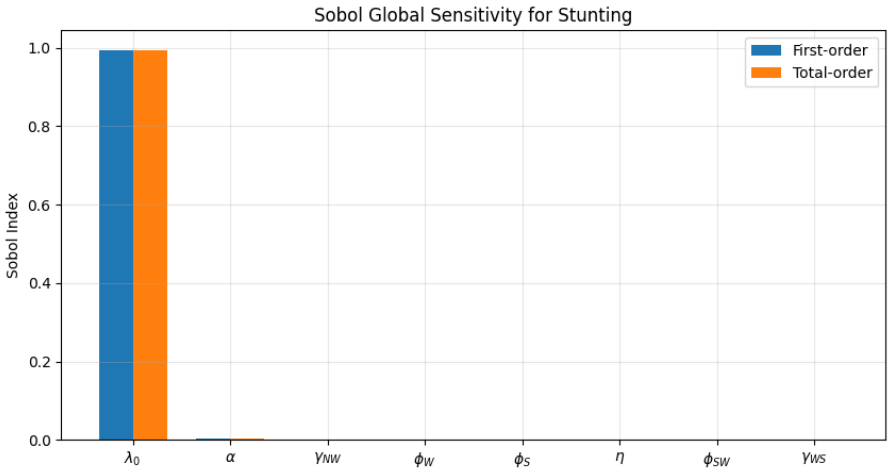

Figure 9. Sobol global sensitivity indices for stunting prevalence.

The dominance of λ_0 is visually evident in Figure 9, where the Sobol bars corresponding to λ_0 almost completely dominate the variance structure of the system. This result reveals an important structural property of the coupled wasting–stunting model: although wasting and stunting are dynamically linked through the interaction mechanism $\lambda_0(1 + \alpha(W + SW))$, the persistence of chronic undernutrition at the population level remains fundamentally controlled by the baseline chronic progression intensity.

Biologically, this finding suggests that chronic growth failure evolves predominantly through slow cumulative structural mechanisms operating over long temporal scales. Such mechanisms may include persistent dietary insufficiency, recurrent infections, maternal nutritional conditions, household food insecurity, environmental enteropathy, sanitation deficits, and long-term socioeconomic vulnerability. Consequently, even substantial short-term reductions in wasting prevalence may generate only limited immediate changes in long-term stunting burden.

The wasting amplification parameter α generated only a small contribution, $S_1 = 0.0038$, indicating that wasting-related amplification contributes only weakly to overall variance in chronic undernutrition prevalence. Nevertheless, the nonzero contribution of α remains biologically meaningful because it confirms the existence of a measurable interaction pathway linking acute malnutrition exposure to chronic growth deterioration.

Importantly, however, the relatively small Sobol magnitude associated with α demonstrates that wasting acts primarily as a secondary amplification mechanism rather than the dominant driver of endemic stunting persistence. In other words, wasting exposure may accelerate or exacerbate chronic undernutrition, but the long-term maintenance of stunting prevalence remains governed primarily by structural chronic progression dynamics.

Similarly, the wasting progression parameter γ_{NW} and wasting recovery parameter ϕ_W generated extremely small Sobol contributions, $S_1 = 0.0007$ and $S_1 = 0.0003$, respectively. These results indicate that uncertainty in acute malnutrition dynamics contributes minimally to long-term variance in chronic growth failure at the population scale. The stunting recovery parameter ϕ_S also generated only a negligible contribution, $S_1 = 0.0001$, which suggests that uncertainty in the calibrated recovery intensity exerts relatively limited influence on overall long-term stunting variance under the present parameter regime. This finding is particularly important because it implies that modest improvements in therapeutic recovery alone may be insufficient to substantially alter chronic undernutrition persistence unless accompanied by broader structural reductions in baseline chronic progression. Meanwhile, the remaining parameters η, ϕ_{SW}, and γ_{WS} produced essentially zero Sobol contributions, indicating that downstream severe wasting dynamics exert minimal direct control over the asymptotic behavior of chronic undernutrition prevalence.

Another important structural feature is the near equivalence between the first-order and total-order Sobol indices for λ_0: $S_1 \approx S_T$. This indicates that higher-order nonlinear interactions contribute negligibly to overall stunting variance. Consequently, the chronic undernutrition subsystem behaves as a highly concentrated and structurally dominated dynamical process rather than an interaction-dominated nonlinear system. From a systems perspective, this result reveals a strong asymmetry in the coupled wasting–stunting dynamics. Wasting prevalence is highly responsive to direct deterioration and recovery processes, whereas stunting prevalence evolves much more slowly through dominant baseline structural progression mechanisms. The wasting subsystem therefore behaves as a relatively reactive acute process, while the stunting subsystem behaves as a persistent structural process with substantially greater temporal inertia.

Overall, the global sensitivity analysis demonstrates that long-term stunting persistence is regulated overwhelmingly by baseline chronic progression dynamics, whereas wasting-related mechanisms contribute only weak secondary amplification effects. These findings remain fully consistent with the threshold sensitivity analysis, local sensitivity analysis, theoretical stability results, calibration results, and long-term numerical projections, collectively supporting the hierarchical structure of the proposed wasting–stunting dynamical system.

5.7. Global sensitivity analysis of the wasting progression threshold

Variance-based Sobol global sensitivity analysis was performed to quantify the relative contribution of parameter uncertainty to the wasting progression threshold

$$\mathcal{R}_W = \frac{\gamma_{NW}(1+\eta s^*)(1-q_W)}{\mu+\delta+\phi_W}.$$

Unlike local sensitivity analysis, which evaluates infinitesimal perturbations around a single calibrated parameter set, Sobol analysis evaluates parameter influence over the entire admissible parameter space while simultaneously accounting for nonlinear and interaction effects.

The first-order Sobol index

$$S_i = \frac{\mathrm{Var}_{X_i}\left(\mathbb{E}[Y|X_i]\right)}{\mathrm{Var}(Y)}$$

measures the direct contribution of parameter X_i to output variance, whereas the total-order index S_{T_i} captures the combined contribution of both direct and higher-order interaction effects. Table 10 and Figure 10 show that the wasting progression threshold $\mathcal{R}_W$ is governed primarily by the wasting deterioration parameter γ_{NW}, which generated $S_1 = 0.7937, \quad S_T = 0.7964$. These results indicate that the majority of the threshold variance originates directly from uncertainty in the nutritional deterioration process from the normal nutritional state into wasting conditions. The dominant contribution of γ_{NW} indicates that wasting persistence is regulated primarily by nutritional deterioration processes. Biologically, this implies that long-term wasting persistence depends mainly on the rate at which nutritionally vulnerable children deteriorate into acute malnutrition rather than on downstream interaction mechanisms.

Table 10. Sobol global sensitivity indices for $\mathcal{R}_W$.

Parameter	S_1	S_T
γ_{NW}	0.7937	0.7964
ϕ_W	0.1893	0.1914
η	0.0068	0.0066
s^*	0.0068	0.0066
q_W	0.0013	0.0012

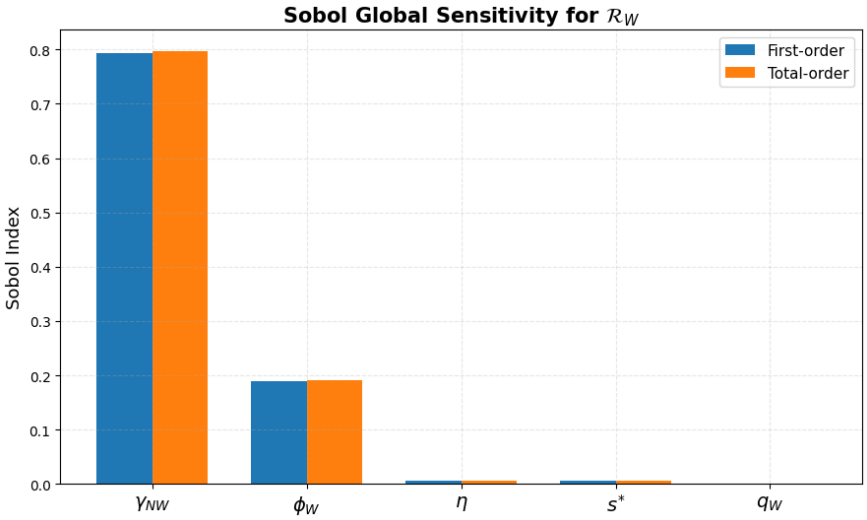

Figure 10. Sobol global sensitivity indices for $\mathcal{R}_W$.

The wasting recovery parameter ϕ_W produced the second-largest contribution, $S_1 = 0.1893, \quad S_T = 0.1914$, confirming its major stabilizing role within the wasting subsystem. Together, γ_{NW} and ϕ_W account for nearly the entire variance structure of $\mathcal{R}_W$. This reveals a highly concentrated regulatory structure in which wasting persistence is governed predominantly by the antagonistic balance between nutritional deterioration and recovery processes.

The interaction parameter η and the endemic stunting level s^* generated identical Sobol contributions, $S_1 = 0.0068$, reflecting the multiplicative interaction structure $(1 + \eta s^*)$ embedded within the threshold formulation.

Biologically, these results indicate the presence of a weak amplification mechanism linking chronic undernutrition to increased wasting persistence. Higher endemic stunting prevalence increases susceptibility to wasting deterioration, thereby slightly elevating the effective wasting threshold. Nevertheless, the relatively small Sobol magnitudes associated with η and s^* indicate that chronic undernutrition acts primarily as a secondary amplification pathway rather than the dominant determinant of wasting persistence.

The low birth weight recruitment parameter q_W generated only a negligible contribution, $S_1 = 0.0013$, indicating that uncertainty in baseline recruitment composition contributes minimally to overall threshold uncertainty compared with postnatal deterioration and recovery processes. Another important structural feature is the near equivalence between first-order and total-order indices $S_1 \approx S_T$. This indicates that higher-order nonlinear interactions contribute minimally to threshold uncertainty. Consequently, the wasting threshold is governed primarily by direct parameter effects rather than complex interaction cascades.

Overall, the Sobol global sensitivity analysis confirms the hierarchical regulatory structure identified throughout the analytical and numerical investigations. Wasting persistence is governed primarily by acute nutritional

deterioration and recovery mechanisms, whereas chronic undernutrition contributes only weak secondary amplification effects through the wasting–stunting interaction pathway.

5.8. Long-term projection simulation

The intervention scenarios considered in this study were constructed based on the current national nutritional policy framework and long-term development targets established by the Government of Indonesia, particularly the RPJMN 2025–2029, the National Strategy for Stunting Reduction, and the long-term human development vision toward Indonesia Emas 2045. These policy frameworks emphasize accelerated reduction of wasting and stunting prevalence through strengthening nutritional rehabilitation programs, supplementary feeding interventions, treatment access, maternal–child nutrition services, and integrated community-based nutritional management systems.

Consistent with the RPJPN 2025–2045 framework, the simulation horizon was extended until 2045 to evaluate the long-term nutritional dynamics under sustained intervention improvements. The intervention scenarios were implemented through proportional increases in the recovery-related parameters ϕ_W, ϕ_{SW}, and ϕ_S, which collectively represent the effective recovery intensity from wasting, severe wasting, and chronic stunting conditions within the population.

Within the proposed dynamical framework, these recovery parameters describe transition intensities governing movement from undernourished states toward improved nutritional conditions. Consequently, increases in recovery intensity should not be interpreted simply as increases in PMT participation alone. Rather, they represent overall improvements in the effectiveness of nutritional recovery processes at the population level.

Operationally, improvements in recovery intensity may arise through multiple mechanisms, including expansion of PMT coverage, improved treatment adherence, earlier nutritional screening, strengthened referral systems, enhanced rehabilitation effectiveness, improved continuity of care, and better integration between community nutrition services and healthcare facilities.

Three intervention scenarios were considered:

1. **Baseline scenario.** The baseline scenario assumes continuation of the current nutritional intervention performance calibrated from the most recent national prevalence and recovery data. Under this scenario, all recovery-related parameters remain fixed at their calibrated baseline values throughout the projection horizon.
2. **Moderate intervention scenario ($+25\%$).** This scenario assumes a 25% increase in the effective recovery intensities ϕ_W, ϕ_{SW}, and ϕ_S. Biologically, the scenario represents moderate strengthening of nutritional rehabilitation systems, treatment accessibility, and recovery effectiveness under realistic program expansion conditions.
3. **Intensive intervention scenario ($+50\%$).** This scenario assumes a 50% increase in recovery-related parameters, representing large-scale strengthening of nutritional rehabilitation capacity, treatment continuity, intervention coverage, and integrated nutritional management systems consistent with aggressive long-term nutritional improvement strategies.

Thus, the proportional increases considered in this study should be interpreted as improvements in the overall effectiveness and speed of nutritional recovery dynamics within the population rather than direct assumptions that exactly 25% or 50% more children immediately recover.

Figure 11 presents the projected long-term dynamics of wasting, severe wasting, and stunting prevalence under the baseline, moderate intervention, and intensive intervention scenarios during 2024–2045.

The upper panel of Figure 11 shows that wasting prevalence responds relatively rapidly to increased recovery intensity. Under the baseline scenario, wasting prevalence decreases gradually from approximately 7.0% in 2024 to approximately 6.5% by 2045. Under the moderate intervention scenario, prevalence declines further to approximately 5.85%, while the intensive intervention scenario lowers wasting prevalence to approximately 5.32%. This comparatively rapid response is consistent with the earlier threshold and sensitivity analyses, which identified the deterioration parameter γ_{NW} and the recovery parameter ϕ_W as the principal regulators of wasting dynamics.

Since these parameters directly govern the balance between nutritional deterioration and rehabilitation, increased recovery intensity rapidly modifies the effective transition balance within the wasting subsystem.

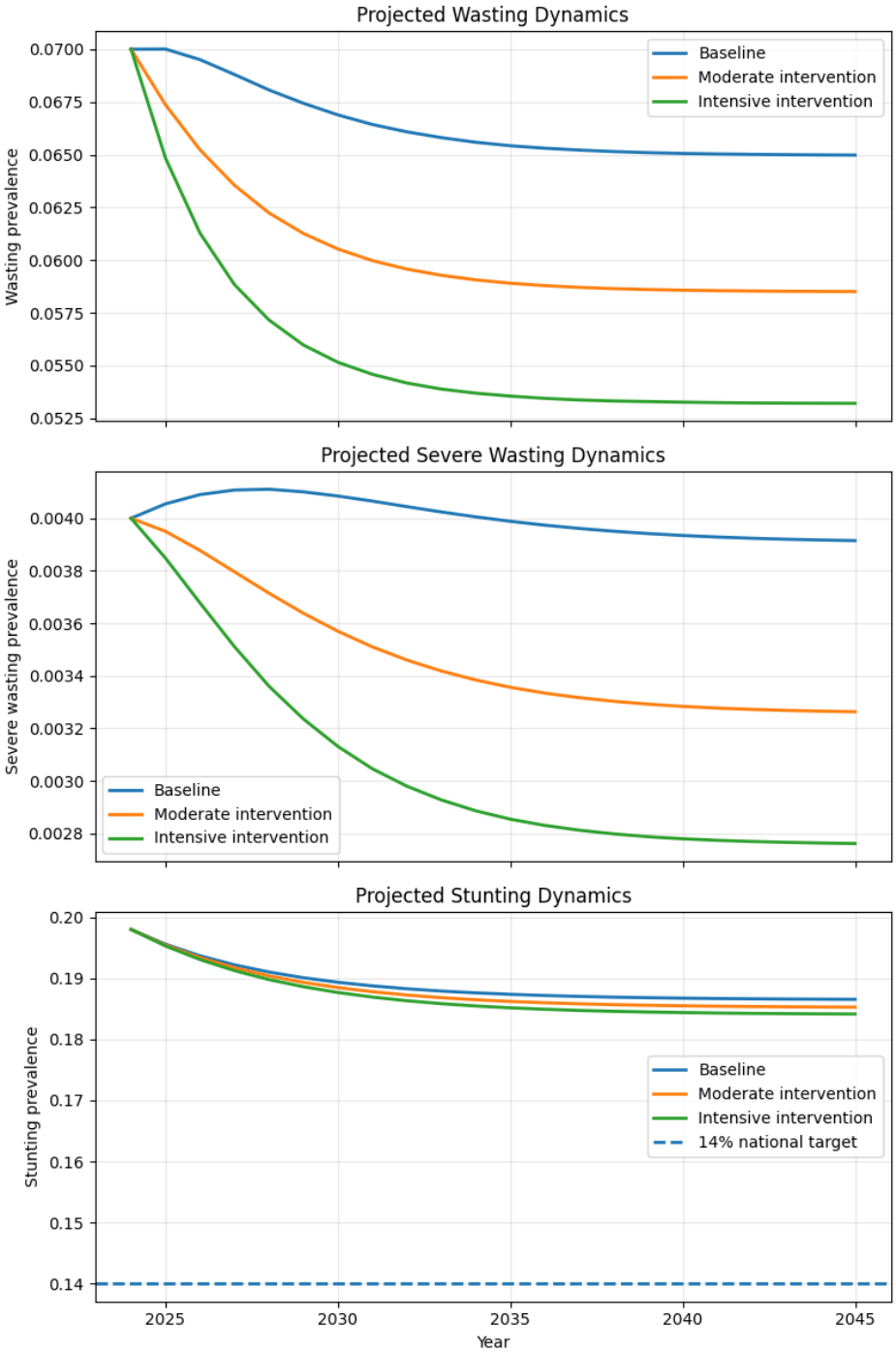

Figure 11. Projected wasting, severe wasting, and stunting prevalence under different intervention scenarios during 2024–2045.

The middle panel of Figure 11 shows that severe wasting prevalence initially exhibits a small transient increase under the baseline scenario before gradually converging toward a stable endemic level near 0.39%. This transient behavior emerges because the inflow from the wasting compartment into severe wasting temporarily exceeds the recovery outflow under baseline recovery intensity. In contrast, both intervention scenarios substantially suppress severe wasting prevalence over time. Under the moderate intervention scenario, severe wasting declines to approximately 0.33% by 2045, whereas the intensive intervention scenario reduces prevalence further to approximately 0.28%. These findings are consistent with the Sobol global sensitivity analysis, which demonstrated that severe wasting dynamics are governed predominantly by progression and recovery processes. Biologically, this indicates that severe acute malnutrition remains highly responsive to improvements in therapeutic rehabilitation and continuity of nutritional management.

The projected stunting dynamics shown in Figure 11 reveal a substantially different long-term behavior. Under the baseline scenario, stunting prevalence declines gradually from approximately 19.8% in 2024 to approximately 18.65% in 2045. Moderate and intensive intervention scenarios accelerate this decline only slightly, reaching approximately 18.53% and 18.42%, respectively, by the end of the projection horizon.

Most importantly, none of the intervention scenarios succeeds in reducing stunting prevalence below the 14% national target threshold by 2045. A particularly important feature of the trajectories is the very small separation between the baseline, moderate, and intensive intervention curves. Even under the intensive intervention scenario corresponding to substantially increased recovery intensity, the long-term reduction in stunting prevalence remains relatively limited. From a dynamical systems perspective, this behavior indicates the presence of strong structural inertia within the chronic undernutrition subsystem. Once chronic growth failure becomes established at the population level, the system converges slowly toward a relatively stable endemic nutritional regime that is resistant to perturbation through recovery-oriented interventions alone. This projection behavior is highly consistent with the earlier sensitivity analyses, which demonstrated that long-term stunting prevalence is governed primarily by the baseline chronic progression parameter λ_0, whereas recovery-related parameters contribute comparatively weaker effects. Epidemiologically, this suggests that chronic undernutrition persistence in Indonesia is driven predominantly by long-duration structural exposure mechanisms rather than short-term nutritional recovery processes alone.

The slow decline of the stunting trajectories also reflects the biological nature of chronic growth failure itself. Unlike wasting, which may respond relatively rapidly to therapeutic feeding and short-term nutritional supplementation, stunting represents cumulative developmental impairment arising from prolonged exposure to inadequate nutrition, recurrent infection, impaired nutrient absorption, maternal undernutrition, poor sanitation, and persistent environmental vulnerability. As a result, reversal of established chronic growth failure occurs substantially more slowly at the population level than recovery from acute malnutrition. The near-flat trajectories after approximately 2035 additionally suggest that the system approaches a stable endemic equilibrium for chronic undernutrition. Intervention-driven recovery initially produces measurable reductions in prevalence, but the rate of decline progressively slows as the system converges toward a structurally persistent equilibrium sustained by underlying environmental and socioeconomic pressures.

Table 11 further highlights two important structural patterns. First, wasting and severe wasting prevalence respond relatively rapidly to increased recovery intensity, particularly under the intensive intervention scenario. Second, reductions in stunting prevalence remain comparatively modest even under substantial intervention strengthening. In particular, although the intensive intervention scenario lowers wasting prevalence from 7.0% to approximately 5.32%, the corresponding reduction in stunting prevalence remains limited, declining only from approximately 19.8% to 18.42% by 2045. Moreover, all nutritional compartments approach near-equilibrium conditions approximately after 2038–2040, beyond which only very small temporal changes remain observable. This convergence pattern suggests that the dominant intervention effects occur primarily during the first decade following intervention strengthening, whereas subsequent dynamics become progressively constrained by the endemic equilibrium structure of the coupled system.

Table 11. Projected nutritional prevalence under different intervention scenarios for selected years during 2024–2045.

	Baseline			Moderate intervention			Intensive intervention		
Year	W	SW	S	W	SW	S	W	SW	S
2024	0.0700	0.0040	0.1980	0.0700	0.0040	0.1980	0.0700	0.0040	0.1980
2030	0.0669	0.0041	0.1893	0.0605	0.0036	0.1885	0.0552	0.0031	0.1877
2035	0.0654	0.0040	0.1874	0.0589	0.0034	0.1862	0.0536	0.0029	0.1852
2040	0.0651	0.0039	0.1867	0.0586	0.0033	0.1855	0.0533	0.0028	0.1844
2045	0.0650	0.0039	0.1865	0.0585	0.0033	0.1853	0.0532	0.0028	0.1842

Another important observation is the absence of oscillatory behavior throughout the projection horizon. Under all intervention scenarios, the coupled system converges smoothly toward stable endemic equilibrium levels. This asymptotic convergence pattern supports the earlier theoretical stability analysis and demonstrates the long-term dynamical consistency of the proposed wasting–stunting model. Overall, the projection trajectories reveal a hierarchical dynamical structure within the coupled system. Acute malnutrition compartments behave as relatively reactive subsystems that respond rapidly to improvements in recovery intensity, whereas chronic undernutrition behaves as a structurally persistent subsystem characterized by slow convergence and strong temporal inertia.

From a policy perspective, these findings suggest that treatment-oriented nutritional programs remain critically important for reducing wasting and severe wasting burden. Nevertheless, substantial long-term reductions in chronic undernutrition likely require broader structural interventions targeting maternal nutrition, household food security, sanitation, environmental health, infection prevention, and early-life developmental conditions in addition to therapeutic nutritional rehabilitation. Overall, the projection analysis reinforces the central conclusion of this study: reductions in acute malnutrition alone are insufficient to rapidly eliminate chronic undernutrition, because long-term stunting persistence is governed predominantly by slow structural nutritional dynamics operating at the population level.

6. Discussion

The present study develops a coupled wasting–stunting dynamical framework integrating acute and chronic undernutrition within a unified population-level system. Unlike conventional nutritional analyses that often treat wasting and stunting as largely independent indicators, the proposed model explicitly incorporates nonlinear interaction mechanisms linking acute nutritional deterioration and chronic growth failure. This structure allows the model to capture how recurrent wasting exposure may amplify long-term stunting persistence, while chronic undernutrition simultaneously increases susceptibility to subsequent wasting progression. Previous epidemiological studies have consistently reported strong associations between wasting and stunting, including elevated risks of concurrent undernutrition, recurrent wasting episodes, impaired catch-up growth, and increased mortality among children experiencing multiple nutritional deficits simultaneously [16]. However, many existing studies remain primarily observational and therefore provide limited insight into the long-term dynamical mechanisms governing nutritional persistence at the population level. In contrast, the present framework demonstrates analytically that wasting acts as an important upstream mechanism capable of amplifying chronic undernutrition dynamics through coupled interaction pathways.

The threshold analysis revealed a hierarchical dynamical structure centered on the wasting progression threshold $\mathcal{R}_W$. The local and global sensitivity analyses demonstrated that this threshold is governed primarily by the wasting deterioration parameter γ_{NW} and the wasting recovery parameter ϕ_W, indicating that the balance between nutritional deterioration and recovery regulates the principal persistence mechanism of the wasting subsystem. An important consistency emerges between the analytical threshold results and the numerical projection dynamics. The calibrated wasting progression threshold satisfied $\mathcal{R}_W < 1$, indicating that wasting amplification remains

dynamically subcritical under the estimated parameter configuration. This theoretical prediction is strongly supported by the long-term simulation trajectories, which showed gradual monotonic decline of wasting and severe wasting prevalence under all intervention scenarios.

Importantly, the simulations did not exhibit explosive wasting growth, oscillatory instability, or sustained acceleration of acute malnutrition prevalence. Instead, both wasting and severe wasting trajectories remained bounded and progressively stabilized over time, consistent with the local stability result established for the wasting-free equilibrium. Nevertheless, complete elimination was not observed within the finite simulation horizon considered in the present study. This behavior remains fully consistent with the theoretical threshold result because the condition $\mathcal{R}_W < 1$, governs the asymptotic long-term dynamics of the wasting subsystem as $t \to \infty$, whereas the numerical projections were restricted to the period 2024–2045. Consequently, although wasting and severe wasting prevalence decline monotonically toward the wasting-free equilibrium, the convergence process occurs gradually over long temporal scales. Within realistic policy horizons, substantial prevalence may therefore remain observable despite the underlying asymptotic stability of the wasting subsystem. This distinction is important epidemiologically. In the present framework, the threshold $\mathcal{R}_W$ represents the long-term amplification potential of acute nutritional deterioration. When $\mathcal{R}_W < 1$, the wasting subsystem becomes asymptotically stable and wasting prevalence gradually declines toward elimination. However, because convergence occurs slowly relative to realistic intervention horizons, measurable wasting prevalence may still persist over several decades before approaching negligible levels.

Biologically, these findings are highly relevant because chronic undernutrition is known to impair immune competence, intestinal absorption, metabolic resilience, and resistance to infectious stressors [35, 36]. Consequently, chronically undernourished children frequently exhibit increased vulnerability to recurrent wasting episodes, thereby generating a reinforcing nutritional deterioration cycle. The positive contribution of η to $\mathcal{R}_W$ further suggests that persistent chronic growth failure may indirectly strengthen wasting persistence by increasing susceptibility to acute nutritional deterioration. This interpretation extends previous conceptual frameworks in nutritional epidemiology. Conventional intervention models frequently assume that wasting and stunting represent parallel but largely independent nutritional outcomes. The present results instead suggest that persistent wasting exposure may continuously activate amplification pathways sustaining chronic growth failure. In particular, the interaction parameter α increases the effective incidence of stunting under persistent wasting exposure, implying that repeated acute nutritional insults may gradually accumulate into long-term developmental impairment even when individual wasting episodes appear clinically resolved. This mechanism provides a plausible explanation for an important phenomenon frequently observed in national nutritional programs: reductions in wasting prevalence do not necessarily produce immediate proportional reductions in stunting prevalence. The model suggests that this delay emerges intrinsically from the cumulative nature of chronic nutritional injury. Since stunting dynamics integrate the long-term history of nutritional exposure, chronic undernutrition may remain persistent even after short-term improvements in acute malnutrition indicators.

The sensitivity analyses strongly reinforce this interpretation. The Sobol global sensitivity analysis demonstrated that wasting prevalence was governed predominantly by the deterioration parameter γ_{NW} and the recovery parameter ϕ_W, whereas severe wasting dynamics were controlled primarily by progression and recovery mechanisms. In contrast, long-term stunting prevalence was dominated primarily by the baseline chronic progression parameter λ_0, while interaction parameters contributed only comparatively weak secondary amplification effects. Importantly, the consistently small differences between first-order and total-order Sobol indices indicate that the proposed nutritional system is governed primarily by direct structural mechanisms rather than highly complex higher-order nonlinear interactions. Epidemiologically, this finding suggests that long-term nutritional persistence may depend predominantly on a limited number of structurally important intervention pathways. The dominance of λ_0 within the stunting subsystem is particularly important biologically and epidemiologically. The parameter λ_0 represents the baseline chronic progression intensity independent of short-term acute nutritional fluctuations. Consequently, the global sensitivity results suggest that long-term stunting persistence in Indonesia is governed primarily by sustained structural exposure processes rather than transient wasting episodes alone. This interpretation is consistent with evidence indicating that chronic growth failure emerges cumulatively through prolonged exposure to inadequate nutrition, recurrent infection,

poor sanitation, maternal undernutrition, and persistent socioeconomic vulnerability operating throughout early childhood development. At the population level, recovery dynamics depend not only on therapeutic nutritional improvement itself, but also on a substantially broader set of mechanisms, including intervention coverage, delayed diagnosis, treatment accessibility, referral continuity, household compliance, environmental sanitation, infection burden, and intergenerational nutritional vulnerability. Consequently, effective population-level recovery intensity may differ substantially from short-term therapeutic recovery observed under controlled clinical settings. An especially important implication of the calibration process concerns the extremely small effective magnitude of the stunting recovery parameter ϕ_S. Unlike wasting recovery, which may occur relatively rapidly after short-term nutritional rehabilitation, chronic growth failure represents cumulative developmental impairment that is substantially more difficult to reverse at the population level. Biologically, this result is highly plausible because linear growth restriction reflects prolonged exposure to nutritional deficiency, recurrent infection, impaired intestinal absorption, maternal undernutrition, environmental enteric dysfunction, and persistent socioeconomic vulnerability accumulated throughout critical developmental periods. Consequently, even when nutritional interventions improve short-term dietary intake, the effective population-level reversal of established chronic growth failure remains intrinsically slow.

The long-term projection results strongly support this interpretation. Under the baseline scenario, stunting prevalence decreased from approximately 19.8% in 2024 to approximately 18.65% by 2045. Under the moderate intervention scenario, prevalence decreased only to approximately 18.53%, while under the intensive intervention scenario corresponding to a 50% increase in recovery-related parameters, the projected prevalence decreased merely to approximately 18.42%. Thus, substantial strengthening of nutritional recovery dynamics produced only marginal displacement of the long-term stunting equilibrium. The small separation between the baseline and intensive intervention trajectories indicates that chronic undernutrition persistence cannot be explained solely by insufficient therapeutic recovery effort, but instead reflects deeper structural mechanisms sustaining long-term developmental vulnerability. Importantly, this asymptotic behavior differs fundamentally from the stunting subsystem. While wasting and severe wasting prevalence gradually decline toward elimination under $\mathcal{R}_W < 1$, the stunting compartment converges toward a strictly positive endemic equilibrium determined primarily by the balance between baseline chronic progression and recovery dynamics. Consequently, the model predicts that acute malnutrition may eventually become controllable over sufficiently long time horizons, whereas chronic undernutrition remains structurally persistent at the population level. From a dynamical systems perspective, these projection trajectories indicate the presence of strong structural inertia within the chronic undernutrition subsystem. Once chronic growth failure becomes established at the population level, the system converges slowly toward a stable endemic nutritional regime that responds only modestly to recovery-oriented intervention strengthening. Importantly, the projection results additionally showed that the national target of reducing stunting prevalence below 14% was not achieved by 2045 under any intervention scenario considered in the present study. Even under intensive recovery enhancement, the predicted prevalence remained substantially above the policy target threshold. This finding further supports the interpretation that chronic undernutrition persistence in Indonesia is sustained by long-duration structural mechanisms that cannot be rapidly displaced through recovery acceleration alone. Nevertheless, the projection results also demonstrated that recovery-oriented interventions remain highly beneficial for reducing acute malnutrition burden. Both wasting and severe wasting prevalence declined substantially under moderate and intensive intervention scenarios, indicating that nutritional rehabilitation programs continue to play an essential role in reducing acute nutritional deterioration and severe morbidity risk at the population level.

Consequently, the present findings should not be interpreted as evidence that nutritional interventions are ineffective, but rather that chronic undernutrition reduction requires substantially longer time horizons and broader structural improvements beyond short-term recovery acceleration alone. The model instead suggests that nutritional interventions generate major public health benefits primarily through reduction of acute nutritional deterioration, prevention of severe morbidity progression, and partial suppression of the amplification pathways linking wasting persistence to chronic growth failure. This interpretation is highly relevant for understanding the persistent difficulty of achieving rapid national stunting reduction in Indonesia despite large-scale expansion of nutritional intervention programs in recent years. Although supplementary feeding programs, nutritional rehabilitation

services, and maternal–child health interventions may substantially reduce acute malnutrition burden, the long-term equilibrium structure of chronic undernutrition remains governed predominantly by persistent structural determinants operating throughout early childhood development.

These determinants likely include household food insecurity, maternal nutritional deficiency, recurrent infectious exposure, sanitation limitations, inadequate dietary diversity, environmental enteric dysfunction, low birth weight prevalence, poverty-related vulnerability, and unequal healthcare accessibility across regions. Because these mechanisms operate cumulatively over long developmental periods, improvements in therapeutic recovery alone may remain insufficient to substantially shift the endemic chronic undernutrition equilibrium.

Importantly, the model also suggests that intervention continuity may be as important as intervention intensity itself. Because chronic undernutrition emerges through cumulative exposure processes, intermittent or short-term nutritional programs may fail to sufficiently disrupt the wasting–stunting amplification cycle [33]. In contrast, sustained prevention of early wasting progression may generate larger long-term reductions in chronic growth failure by suppressing the upstream mechanisms responsible for activating chronic amplification pathways [51]. This interpretation is also consistent with developmental biology evidence indicating that the first 1000 days of life constitute a critical physiological window during which repeated nutritional insults may produce long-lasting effects on growth trajectory, neurodevelopment, immune competence, and metabolic regulation [33, 35]. Once chronic growth impairment becomes established, complete reversal may become progressively more difficult despite later nutritional rehabilitation [33]. Consequently, prevention of early wasting progression may produce greater long-term population impact than downstream treatment of severe chronic impairment after prolonged exposure has already occurred.

Several limitations should nevertheless be acknowledged. Because the model was calibrated primarily using aggregate national prevalence trajectories rather than longitudinal individual transition observations, several estimated parameters should be interpreted as effective population-level quantities rather than direct biological transition rates. Consequently, the derived thresholds represent effective dynamical persistence indicators at the population scale rather than exact physiological reproduction mechanisms in the classical infectious disease sense. In addition, the model does not explicitly incorporate spatial heterogeneity, household behavioral variability, socioeconomic stratification, infection-specific dynamics, or regional disparities in nutritional service accessibility. Several interaction parameters additionally remain semi-mechanistic because of limited availability of longitudinal nutritional transition datasets. Consequently, the coupled amplification structure should be interpreted primarily as an effective epidemiological representation rather than a direct physiological causal pathway at the individual level. Nevertheless, the consistency between the theoretical threshold structure, calibration behavior, profile likelihood analysis, local and global sensitivity analyses, and long-term projection dynamics suggests that the model successfully captures the dominant large-scale mechanisms governing wasting–stunting persistence within the Indonesian nutritional system.

Overall, the present study suggests that chronic undernutrition should not be interpreted merely as a static nutritional endpoint, but rather as an emergent population-level consequence of sustained nutritional exposure and long-term feedback accumulation. The results indicate that long-term stunting persistence in Indonesia is governed predominantly by slow structural nutritional dynamics operating continuously throughout early childhood development. Consequently, substantial long-term reduction of chronic undernutrition likely requires not only nutritional rehabilitation programs, but also sustained multisectoral structural transformation targeting the upstream determinants continuously reinforcing chronic developmental vulnerability.

7. Conclusion

This study developed a coupled wasting–stunting dynamical model describing the interaction between acute and chronic undernutrition among children under five years of age. Unlike conventional nutritional models that treat wasting and stunting as independent epidemiological outcomes, the proposed framework explicitly incorporates nonlinear interaction mechanisms linking acute nutritional deterioration and long-term chronic growth failure within a unified population-level system.

The analytical results revealed that the wasting subsystem governs the principal threshold structure of the model through the wasting progression threshold $\mathcal{R}_W$. The analysis demonstrated that persistent wasting exposure may continuously activate amplification pathways sustaining chronic undernutrition persistence, while chronic growth failure simultaneously increases susceptibility to recurrent wasting progression. Consequently, the coupled system exhibits a hierarchical nonlinear feedback structure in which acute and chronic undernutrition reinforce one another over extended developmental time scales.

The local and global sensitivity analyses strongly supported these theoretical findings. Wasting prevalence was governed predominantly by the deterioration parameter γ_{NW} and the recovery parameter ϕ_W, whereas severe wasting dynamics were controlled primarily by progression and recovery processes. In contrast, long-term stunting prevalence was dominated primarily by the baseline chronic progression parameter λ_0, while interaction parameters contributed only comparatively weak secondary amplification effects. The relatively small differences between first-order and total-order Sobol indices further indicated that the nutritional system is governed mainly by a limited number of structurally dominant mechanisms rather than highly diffuse higher-order nonlinear interactions.

An important consistency emerged between the analytical threshold results and the numerical projection dynamics. The calibrated parameter configuration satisfied $\mathcal{R}_W < 1$, indicating that the wasting subsystem remains asymptotically stable over long time horizons. This theoretical prediction was consistent with the simulation trajectories, which showed gradual monotonic decline of wasting and severe wasting prevalence under all intervention scenarios. Nevertheless, complete elimination was not observed within the projection horizon 2024–2045, indicating that convergence toward the wasting-free equilibrium occurs relatively slowly at the population level.

An especially important implication of the calibration process concerns the extremely small effective magnitude of the stunting recovery parameter ϕ_S. The resulting long-term dynamics suggest that chronic growth failure behaves fundamentally differently from acute malnutrition recovery at the population level. Whereas wasting may respond relatively rapidly to nutritional rehabilitation, chronic undernutrition exhibits substantially slower recovery dynamics because it reflects cumulative long-duration developmental impairment sustained by persistent nutritional, environmental, infectious, and socioeconomic pressures.

The long-term numerical projections further demonstrated that even substantial increases in recovery-related intervention intensity produced only marginal reductions in stunting prevalence. Under the intensive intervention scenario corresponding to a 50% increase in recovery-related parameters, the projected stunting prevalence in 2045 remained above 18%, substantially higher than the national target threshold of 14%. These findings indicate the presence of strong structural inertia within the chronic undernutrition subsystem and suggest that long-term stunting persistence in Indonesia is governed predominantly by deep structural mechanisms rather than by short-term therapeutic recovery limitations alone.

Importantly, the projection results also demonstrated that nutritional interventions remain highly beneficial for reducing acute malnutrition burden. Both wasting and severe wasting prevalence declined substantially under moderate and intensive intervention scenarios, indicating that recovery-oriented nutritional programs continue to play an essential role in reducing acute nutritional deterioration and severe morbidity risk at the population level. Consequently, the present findings should not be interpreted as evidence that nutritional interventions are ineffective, but rather that chronic undernutrition reduction requires substantially longer time horizons and broader structural transformation processes beyond short-term recovery acceleration alone.

From a public health perspective, the model suggests that prevention of early wasting progression may generate substantially larger long-term reductions in chronic undernutrition than downstream treatment of severe nutritional impairment alone. Interventions targeting wasting prevention not only reduce acute nutritional deterioration directly, but also suppress the nonlinear amplification pathways sustaining long-term chronic growth failure. However, the projection results additionally suggest that therapeutic nutritional recovery alone may remain insufficient to substantially shift the endemic chronic undernutrition equilibrium without broader structural improvements addressing maternal nutrition, household food security, sanitation, environmental health, infection prevention, and persistent socioeconomic vulnerability.

Although the proposed framework remains limited by the use of aggregate prevalence observations and several semi-mechanistic assumptions, the consistency between the theoretical threshold structure, calibration behavior,

profile likelihood analysis, sensitivity analyses, and long-term projection dynamics suggests that the model successfully captures the dominant large-scale mechanisms governing wasting–stunting persistence within the Indonesian nutritional system.

More broadly, the present study suggests that chronic undernutrition should not be interpreted merely as a static nutritional endpoint, but rather as an emergent population-level consequence of sustained nutritional exposure and long-term feedback accumulation. Within this perspective, persistent wasting exposure may continuously reshape future nutritional vulnerability at the population level, thereby generating chronic growth failure that remains difficult to reverse even after visible short-term clinical improvement has been achieved.

Overall, the study provides a unified theoretical and computational framework linking threshold analysis, nonlinear nutritional interaction dynamics, semi-mechanistic calibration, local and global sensitivity analysis, and long-term policy projection within a single mathematical structure. The proposed framework therefore offers a quantitative basis for evaluating realistic long-term nutritional intervention strategies using routinely collected surveillance data in settings where detailed longitudinal nutritional transition observations remain limited.

Future research may extend the proposed framework by incorporating spatial heterogeneity, age-structured nutritional progression, household-level socioeconomic variability, and optimal intervention allocation strategies. Integration of longitudinal nutritional transition datasets may additionally improve estimation of recovery dynamics and strengthen practical identifiability of several semi-mechanistic parameters. Such extensions may provide a more detailed understanding of regional nutritional persistence and support the development of more targeted long-term nutritional intervention policies.

Acknowledgement

The authors gratefully acknowledge the financial support provided by the Direktorat Penelitian dan Pengabdian kepada Masyarakat, Direktorat Jenderal Riset dan Pengembangan, Kementerian Pendidikan Tinggi, Sains, dan Teknologi Republik Indonesia through the Penelitian Dosen Pemula research grant scheme. This support made the completion of this research possible.

REFERENCES

1. World Health Organization, *WHO guideline on the prevention and management of wasting and nutritional oedema (acute malnutrition) in infants and children under 5 years*, World Health Organization, Geneva, 2023.
2. UNICEF, World Health Organization, and World Bank Group, *Levels and trends in child malnutrition: UNICEF/WHO/World Bank Group joint child malnutrition estimates: key findings of the 2025 edition*, World Health Organization, Geneva, 2025.
3. UNICEF, *The State of Food Security and Nutrition in the World 2025*, Available at: https://data.unicef.org/resources/sofi-2025/ (accessed February 2026).
4. B. Allen, and J. Saunders, *Malnutrition and undernutrition: causes, consequences, assessment and management*, Medicine, vol. 51, no. 7, pp. 461–468, 2023.
5. E. Aydın, M. Tanrıverdi, Ö. Pasin, C. Heybeli, D. A. Kirazoğlu, L. Boyer, M. Rahmati, and P. Soysal, *The impact of malnutrition and associated nutritional deficiencies on mortality in older adults*, Clinical Nutrition ESPEN, vol. 70, pp. 174–181, 2025.
6. Y.-W. Hsu, C.-H. Lu, S.-Y. Chen, H.-W. Kou, Y.-F. Chen, M.-Y. Chen, J.-T. Hsu, K.-Y. Yeh, Y.-S. Hung, and W.-C. Chou, *Prevalence and prognostic impact of malnutrition at cancer diagnosis: A prospective cohort study*, Clinical Nutrition ESPEN, vol. 72, article 102943, 2026.
7. N. Rahmi, and W. Ekasasmita, *A mathematical model to restrain pneumonia spread in children under five years considering nutritional status, household air pollution, vaccination, and health monitoring*, in *The 6th IICMA 2023*, vol. 58, pp. 1–14, 2024.
8. M. Batal, A. Deaconu, and L. Steinhause, *The nutrition transition and the double burden of malnutrition*, in *Nutritional Health*, N. J. Temple, T. Wilson, D. R. Jacobs Jr., and G. A. Bray (eds.), Humana, Cham, 2023.
9. World Health Organization, *Malnutrition in children*, Available at: https://www.who.int/data/nutrition/nlis/info/malnutrition-in-children (accessed February 2026).
10. S. M. Schoenbuchner, C. Dolan, M. Mwangome, A. Hall, S. A. Richard, J. C. Wells, T. Khara, B. Sonko, A. M. Prentice, and S. E. Moore, *The relationship between wasting and stunting: a retrospective cohort analysis of longitudinal data in Gambian children from 1976 to 2016*, The American Journal of Clinical Nutrition, vol. 110, no. 2, pp. 498–507, 2019.
11. A. Hasman, G. Moloney, and V. Aguayo, *Brief guidance note: Age prioritization of nutrition interventions for child survival, growth and development in resource-constrained contexts*, UNICEF, New York, 2024.
12. S. B. Ickes, C. Craig, and R. Heidkamp, *Design factors for food supplementation and nutrition education interventions that limit conclusions about effectiveness for wasting prevention: A scoping review of peer-reviewed literature*, Advances in Nutrition, vol. 13, no. 1, pp. 328–341, 2021.

13. S. Thurstans, N. Sessions, C. Dolan, K. Sadler, B. Cichon, S. Isanaka, D. Roberfroid, H. Stobaugh, P. Webb, and T. Khara, *The relationship between wasting and stunting in young children: A systematic review*, Maternal & Child Nutrition, pp. 1–25, 2021.
14. L. A. Jokhu, and A. Syauqy, *Determinants of concurrent wasting and stunting among children 6 to 23 mo in Indonesia*, Nutrition, vol. 122, article 112390, 2024.
15. S. O. Konyole, S. A. Omollo, J. N. Kinyuru, B. O. Owuor, B. B. Estambale, C. Ritz, K. F. Michaelsen, S. M. Filteau, J. C. Wells, N. Roos, H. Friis, V. O. Owino, and B. Grenov, *Associations between stunting, wasting and body composition: A longitudinal study in 6- to 15-month-old Kenyan children*, The Journal of Nutrition, vol. 153, no. 4, pp. 970–978, 2023.
16. A. Mertens, J. Benjamin-Chung, J. M. Colford Jr, A. E. Hubbard, M. J. van der Laan, J. Coyle, O. Sofrygin, W. Cai, W. Jilek, S. Rosete, A. Nguyen, N. N. Pokpongkiat, S. Djajadi, A. Seth, E. Jung, E. O. Chung, I. Malenica, N. Hejazi, H. Li, R. Hafen, V. Subramoney, T. Norman, P. Christian, K. H. Brown, and B. F. Arnold, *Child wasting and concurrent stunting in low- and middle-income countries*, Nature, vol. 621, no. 7979, pp. 558–567, 2023.
17. M. A. L. Suratri, E. Indriasih, T. S. Warouw, V. A. Edwin, A. Yulianto, D. R. Faizal, N. M. S. Deva, A. Yulianti, T. P. Agus, N. E. Pracoyo, and R. Raharni, *The Relationship between Infectious Diseases and Stunting among Toddlers in Indonesia*, Iranian Journal of Nursing and Midwifery Research, vol. 30, no. 6, pp. 936–940, 2025.
18. I. S. Yamin, S. D. Rahmawati, and B. R. N. Furqan, *The Differential Effect of Community-Based Supplementary Feeding on Wasting and Stunting: Epidemiological Evidence from an Endemic Region in West Nusa Tenggara*, Jurnal Kesehatan Tropis Indonesia, vol. 4, no. 1, pp. 9–17, Jan. 2026.
19. Kementerian Kesehatan Republik Indonesia, *Profil Kesehatan Indonesia Tahun 2022*, Kementerian Kesehatan Republik Indonesia, Jakarta, 2023.
20. Badan Kebijakan Pembangunan Kesehatan, Kementerian Kesehatan Republik Indonesia, *Laporan Survei Kesehatan Indonesia (SKI) 2023 dalam Angka*, Kementerian Kesehatan RI, Jakarta, 2024.
21. Kementerian Kesehatan Republik Indonesia, *Hasil Survei Status Gizi Indonesia (SSGI) 2022*, Kementerian Kesehatan Republik Indonesia, Jakarta, 2022.
22. Badan Kebijakan Pembangunan Kesehatan, Kementerian Kesehatan Republik Indonesia, *Laporan Survei Status Gizi Indonesia (SSGI) 2024*, Kementerian Kesehatan Republik Indonesia, Jakarta, 2025.
23. N. Rahmi, W. Ekasasmita, and A. Fajri, *Analisis matematika dalam pengendalian stunting: pendekatan prevalensi, pemodelan dinamik, dan matematika keuangan*, Indonesia Emas Group, Bandung, 2025.
24. W. Ekasasmita, N. Rahmi, K. Tunnisa, and M. Ikhlashul Amal, *Optimizing defined benefit pension plan funding: combining entry age normal method and single salary approach*, BAREKENG: Jurnal Ilmu Matematika dan Terapan, vol. 19, no. 3, pp. 1553–1564, 2025.
25. H. Husain, Kusnaeni, M. R. Nisardi, Irmayani, N. Rahmi, and A. O. R. M. Rahman, *Nonparametric regression approaches to stunting prevalence: A comparative study of spline truncated and Fourier series*, in *Proceedings of the 5th Borneo International Conference (BICAME 2024)*, pp. 14–22, 2025.
26. D. Azriani, D. Agustian, Y. Zuhairini, I. N. Yulita, and M. Dhamayanti, *Prediction models for stunting at 2-years-old from Indonesian newborn population*, BMC Pediatrics, vol. 25, article 718, 2025.
27. L. O. Sabran, and A. R. Laura, *Dynamic analysis of the mathematical model for stunting with nutrition and education interventions*, BAREKENG: Jurnal Ilmu Matematika dan Terapan, vol. 19, pp. 2317–2334, 2025.
28. E. Faiqotul Himmah, R. Kaestria, and Riana, *Mathematical Modeling of Stunting with the Influence of Nutritional Intervention*, JTAM (Jurnal Teori dan Aplikasi Matematika), vol. 9, no. 1, pp. 54–67, 2025.
29. J. D. Meisel, O. L. Sarmiento, C. Olaya, P. D. Lemoine, J. A. Valdivia, and R. Zarama, *Towards a novel model for studying the nutritional stage dynamics of the Colombian population by age and socioeconomic status*, PLoS ONE, vol. 13, no. 2, article e0191929, 2018.
30. F. Abbas, R. Kumar, T. Mahmood, et al., *Impact of children born with low birth weight on stunting and wasting in Sindh province of Pakistan: a propensity score matching approach*, Scientific Reports, vol. 11, p. 19932, 2021.
31. I. Rahmadiani, A. I. Fibriana, A. A. Nisa, S. A. Shabbir, and M. Azam, *Impact of Low Birth Weight and Other Determinants on Stunting in Children Under-Five Years Old: Evidence from Indonesia's Nutrition Status Survey*, International Journal of Preventive Medicine, vol. 16, p. 76, 2025.
32. S. Das, S. M. Fahim, M. A. Alam, M. Mahfuz, P. Bessong, E. Mduma, M. Kosek, S. K. Shrestha, and T. Ahmed, *Not water, sanitation and hygiene practice, but timing of stunting is associated with recovery from stunting at 24 months: results from a multi-country birth cohort study*, Public Health Nutrition, vol. 24, no. 6, pp. 1428–1437, 2021.
33. S. A. Richard et al., *Influences on catch-up growth using relative versus absolute metrics: evidence from the MAL-ED cohort study*, BMC Public Health, vol. 21, no. 1, p. 1246, 2021. Available at: https://doi.org/10.1186/s12889-021-11120-0.
34. B. Sahiledengle, K. E. Agho, P. Petrucka, A. Kumie, G. Beressa, D. Atlaw, Y. Tekalegn, D. Zenbaba, F. Desta, and L. Mwanri, *Concurrent wasting and stunting among under-five children in the context of Ethiopia: A generalised mixed-effects modelling*, Maternal & Child Nutrition, vol. 19, pp. 1–20, 2023.
35. A. Kirolos, R. M. Blacow, A. Parajuli, N. J. Welton, A. Khanna, S. J. Allen, et al., *The impact of childhood malnutrition on mortality from pneumonia: a systematic review and network meta-analysis*, BMJ Global Health, vol. 6, e007411, 2021. Available at: https://doi.org/10.1136/bmjgh-2021-007411.
36. K. D. Tickell, R. Sharmin, E. L. Deichsel, L. M. Lamberti, J. L. Walson, A. S. G. Faruque, P. B. Pavlinac, K. L. Kotloff, and M. J. Chisti, *The effect of acute malnutrition on enteric pathogens, moderate-to-severe diarrhoea, and associated mortality in the Global Enteric Multicenter Study cohort: a post-hoc analysis*, The Lancet Global Health, vol. 8, no. 2, pp. e215–e224, 2020. Available at: https://doi.org/10.1016/S2214-109X(19)30498-X.
37. A. S. R. Srinivasa Rao and J. R. Carey, *Stationary status of discrete and continuous age-structured population models*, Mathematical Biosciences, vol. 356, article 109058, 2023. Available at: https://doi.org/10.1016/j.mbs.2023.109058.
38. J. R. Carey and A. S. R. Srinivasa Rao, *Stationary Population Dynamics Reveal a Structural Typology of Global Aging: A Binary Model Approach Across 195 Countries*, Research Square, 2025. Available at: https://doi.org/10.21203/rs.3.rs-6675831/v1.

39. P. Mahato, S. K. Mahato, S. Das, and P. Karmakar, *Stationary distribution and density function analysis of SVIS epidemic model with saturated incidence and vaccination under stochastic environments*, Theory in Biosciences, vol. 142, no. 2, pp. 181–198, 2023. Available at: https://doi.org/10.1007/s12064-023-00392-2.
40. H. Cao, X. Liu, and L. Nie, *Extinction and stationary distribution of a novel SIRS epidemic model with general incidence rate and Ornstein–Uhlenbeck process*, Advances in Continuous and Discrete Models, 2024, article 24. Available at: https://doi.org/10.1186/s13662-024-03821-8.
41. Kementerian Kesehatan Republik Indonesia, *Profil Kesehatan Indonesia Tahun 2013*, Kementerian Kesehatan Republik Indonesia, Jakarta, 2014.
42. Kementerian Kesehatan Republik Indonesia, *Profil Kesehatan Indonesia Tahun 2015*, Kementerian Kesehatan Republik Indonesia, Jakarta, 2016.
43. Kementerian Kesehatan Republik Indonesia, *Profil Kesehatan Indonesia Tahun 2016*, Kementerian Kesehatan Republik Indonesia, Jakarta, 2017.
44. Kementerian Kesehatan Republik Indonesia, *Profil Kesehatan Indonesia Tahun 2017*, Kementerian Kesehatan Republik Indonesia, Jakarta, 2018.
45. Kementerian Kesehatan Republik Indonesia, *Profil Kesehatan Indonesia Tahun 2018*, Kementerian Kesehatan Republik Indonesia, Jakarta, 2019.
46. Kementerian Kesehatan Republik Indonesia, *Profil Kesehatan Indonesia Tahun 2019*, Kementerian Kesehatan Republik Indonesia, Jakarta, 2020.
47. Kementerian Kesehatan Republik Indonesia, *Profil Kesehatan Indonesia Tahun 2023*, Kementerian Kesehatan Republik Indonesia, Jakarta, 2024.
48. Kementerian Kesehatan Republik Indonesia, *Profil Kesehatan Indonesia Tahun 2024*, Kementerian Kesehatan Republik Indonesia, Jakarta, 2025.
49. Badan Penelitian dan Pengembangan Kesehatan, Kementerian Kesehatan Republik Indonesia, *Riset Kesehatan Dasar (Riskesdas) Tahun 2018*, Kementerian Kesehatan Republik Indonesia, Jakarta, 2018.
50. Kementerian Kesehatan Republik Indonesia, *Sistem Informasi Gizi Terpadu (SIGIZI): Data hasil intervensi Pemberian Makanan Tambahan (PMT) tahun 2024*, Available at: https://sigizikesga.kemkes.go.id (accessed 2025).
51. D.R. Sjarif, K. Yuliarti, L.C. Gultom, C.N. Hafifah, I.G.L. Sidharta, M. Herdiana Hanindita, N. Nurani, A. Juliaty, et al., *Effectiveness of a Tiered Referral System and Early Nutritional Intervention to Prevent and Recover Stunting in Under-Five Indonesian Children*, Food Science & Nutrition, vol. 13, no. 10, article e70945, 2025. Available at: https://doi.org/10.1002/fsn3.70945.